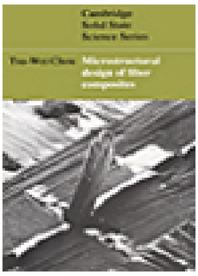

Microstructural Design of Fiber Composites

Tsu-Wei Chou

Book DOI: http://dx.doi.org/10.1017/CBO9780511600272

Online ISBN: 9780511600272

Hardback ISBN: 9780521354820

Paperback ISBN: 9780521019651

Chapter

9 - Nonlinear elastic finite deformation of flexible composites pp. 47
4-525

Chapter DOI: http://dx.doi.org/10.1017/CBO9780511600272.010

Cambridge University Press

9 Nonlinear elastic finite deformation of flexible composites

9.1 Introduction

Flexible composites, which are described in Chapter 8, behave very differently from conventional rigid polymer composites in the following ways:

(1) Flexible composites are highly anisotropic (i.e. longitudinal elastic modulus/transverse elastic modulus $\gg 1$). Figure 9.1 compares the normalized effective Young's modulus (E_{xx}/E_{22}) vs. fiber orientation for two types of unidirectional composites. The upper curve obtained from Kevlar-49/silicone elastomer shows that the stiffness of the elastomeric composite lamina is very sensitive to the fiber orientation. At a 5° off-axis fiber orientation, for example, a 1° change in fiber angle causes the effective stiffness to change by 53%. The lower curve obtained from Kevlar-49/epoxy shows less than 7% change at the same off-axis angle.
(2) Flexible composites show low shear modulus and hence large shear distortion, which allows the fibers to change their orientations under loading.
(3) Flexible composites have a much larger elastic deformation range than that of conventional rigid polymer composites. Thus, the geometric changes of the configuration (i.e. area, direction, etc.) need to be taken into consideration.
(4) The nonlinear elastic behavior with stretching–shear coupling, due to material and geometrical effects, is pronounced in flexible composites under finite deformation.

Therefore, the conventional linear elastic theory, based on the infinitesimal strain assumption for rigid matrix composites, may no longer be applicable to elastomeric composites under finite deformation.

The theories of non-linear and finite elasticity made a major advancement during the Second World War, in response to the development of the rubber industry. M. Mooney, in 1940, advanced his well-known strain–energy function. Rivlin and colleagues (for example, Rivlin 1948a&b; Rivlin and Saunders 1951; Ericksen and

Rivlin 1954), in a series of publications starting in 1948, successfully predicted the large deformation of rubber-like incompressible isotropic material. These works have greatly enhanced and stimulated the development of nonlinear finite elasticity. The fundamental aspects of finite elasticity can be found in advanced text books (for example, Truesdell 1966; Fung 1977; Malvern 1969; Spencer 1972; Lai, Rubin and Krempl 1978).

To predict the large deformation of fiber reinforced rubber material, Adkins and Rivlin (1955) treated the nonlinear, anisotropic, and finite deformation problem by using the 'ideal fiber reinforced material theory'; the assumptions of volume incompressibility and fiber inextensibility are basic to the analysis. Further developments of this theory can be found in the work of Rivlin (1964), Pipkin and Rogers (1971) and Spencer (1972). Difficulties often arise in applying this theory to composites with complicated fiber geometries and in cases where the extension of the fibers cannot be neglected.

Fig. 9.1. Variation of effective Young's modulus with fiber orientation. (After Luo, 1988.)

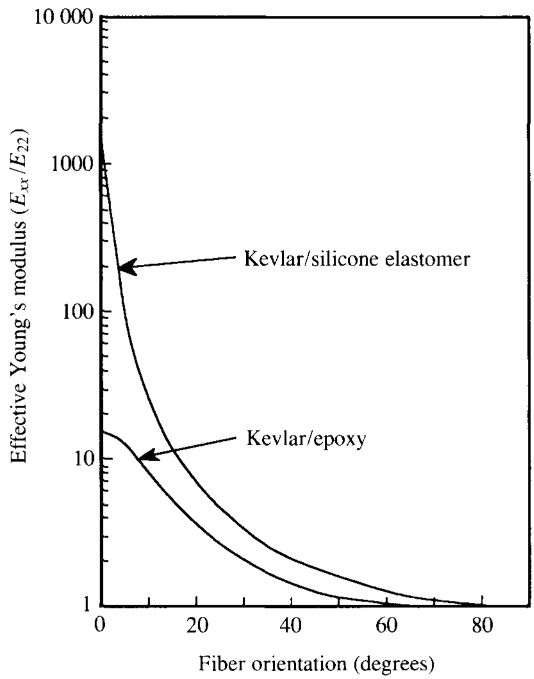

The ability of flexible composites to sustain large deformation and fatigue loading, and still provide high load carrying capacity, has been mainly analyzed in textile cord/rubber composites and coated fabrics. However, most of the existing analyses on the mechanics of pneumatic tires are primarily based on the composite lamination theory for small linear deformation. Chou (1989) has provided a review of the mechanics of flexible composites.

In recent years, the constitutive relation of biological materials has been a subject of considerable research interest. A variety of biological materials are incompressible, viscoelastic, and anisotropic; they often demonstrate nonlinear behavior with a large deformation range (Fung 1981). For instance, Aspden (1986) considered the influences of fiber reorientation in biological materials during finite deformation by using a fiber orientation distribution function and assuming that the fiber carries only axial tension. However, the finite deformation and the rigid body rotation of fibers, as well as the shear property of the matrix material, which greatly influence the fiber reorientation during deformation, are not adequately considered in the analysis. Humphrey and Yin (1987) presented a constitutive model based upon a pseudostrain–energy function, and compared the theoretical analysis with both uniaxial and biaxial experimental results. The parameters used in the energy function are dependent on the experimental data; the fiber spatial arrangements, which are responsible for the geometric nonlinearity, are ignored in their analysis.

Various response functions have been proposed to represent the experimentally determined nonlinear stress–strain curves in principal material directions. Petit and Waddoups (1969) employed the increment method. Hahn (1973) and Hahn and Tsai (1973) used the complementary energy density to derive the stress–strain relation, which is nonlinear in shear but linear in tensile properties. Jones and Morgan (1977) used an orthotropic material model in which the nonlinear mechanical properties are functions of the elastic energy density. The nonlinear elastic behavior of textile structural composites has been examined by Ishikawa and Chou (1983). However, these analyses are restricted to a small strain range.

In an effort to provide a rigorous treatment of the finite deformation problem, two analytical approaches, considering both geometric and material nonlinearities, have been employed in this chapter to predict the constitutive relations of flexible composites (R. S. Rivlin, private communication, 1986; Luo and Chou, 1988a, 1990a&b).

(1) In the first method (Section 9.3), a closed form representation of the constitutive equations has been derived based on the Lagrangian description. The strain–energy density is assumed to be a function of the Lagrangian strain components referring to the initial principal material coordinate $\bar{X}$ (Fig. 9.2a).

(2) In the second approach (Section 9.4), a nonlinear constitutive relation has also been developed based upon the Eulerian description where the deformed configuration of the composite is used as the reference state. A stress–energy function, referring to the moving principal material

Fig. 9.2. A rectangular element of composite lamina before and after loading (a) in the Lagrangian system, (b) in the Eulerian system. (After Luo and Chou 1988a.)

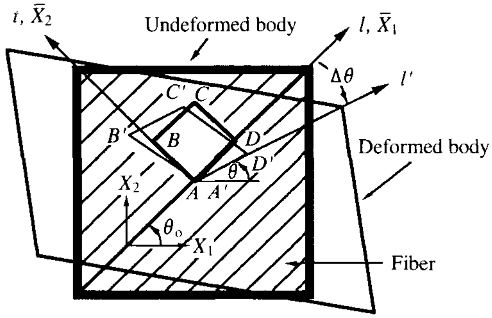

(a)

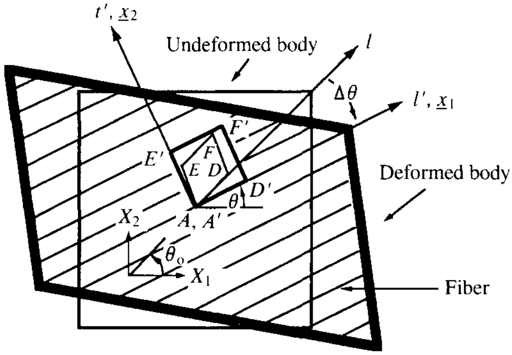

(b)

coordinate $\underset{\sim}{x}$ (Fig. 9.2b), provides the basis for deriving the constitutive relations; and an iterative calculation method is employed.

The constitutive relations obtained from Sections 9.3 and 9.4 have been applied to study the nonlinear elastic behavior of flexible composites with wavy fibers in Section 9.5. Section 9.2, which is based upon Luo (1988), provides the basis for the theoretical treatment of this chapter.

9.2 Background

9.2.1 *Tensor notation*

Some brief descriptions of the notations and operations of tensors are shown in this section. These are taken from various sources, including Fung (1965, 1977), Rivlin (1970) and Lai, Rubin and Krempl (1978). It is not intended to provide a comprehensive coverage of tensor analysis. Only the subjects that are relevant to the present work are described. For simplicity, only Cartesian tensors are used, and thus the distinction between contravariance and covariance disappears and all indices of the tensor components can be written as subscripts. Furthermore, tensors are printed in bold-faced letters.

Einstein summation convention

The following three equations have the same meaning:

$$\begin{aligned} y_i &= a_{ij}x_j \\ &= \sum_{j=1}^{n} a_{ij}x_j \\ &= a_{i1}x_1 + a_{i2}x_2 + a_{i3}x_3 + \cdots + a_{in}x_n \end{aligned} \tag{9.1}$$

The first line of Eq. (9.1) follows the rule of Einstein summation. Here, j is known as the dummy index, which repeats once, denoting a summation with respect to that index over its range, and i is a free index, which appears once in every term of the equation, assuming the numbers of 1, 2 or 3. The following are two other examples:

(1) For the two vectors $\mathbf{a} = a_i\mathbf{e}_i$, and $\mathbf{b} = b_i\mathbf{e}_i$ $(i = 1,2,3)$, the scalar product is defined by

$$c = \mathbf{a} \cdot \mathbf{b} = \sum_{i=1}^{3}\sum_{j=1}^{3} a_i b_j(\mathbf{e}_i \cdot \mathbf{e}_j) \equiv a_i b_j(\mathbf{e}_i \cdot \mathbf{e}_j) \tag{9.2}$$

(2) For the matrices $\mathbf{a} = [a_{ij}]$ and $\mathbf{b} = [b_{ij}]$ $(i = 1,2,3,\ j = 1,2,3)$, the product of these two matrices is

$$[c_{ij}] = \mathbf{ab} = \sum_{k=1}^{3} [a_{ik} b_{kj}] \equiv [a_{ik} b_{kj}] \tag{9.3}$$

Kronecker delta

The Kronecker delta δ is defined as

$$\delta_{ij} = \begin{cases} 1 & \text{for } i = j \\ 0 & \text{for } i \neq j \end{cases} \tag{9.4}$$

or

$$\delta = \begin{bmatrix} \delta_{11} & \delta_{12} & \delta_{13} \\ \delta_{21} & \delta_{22} & \delta_{23} \\ \delta_{31} & \delta_{32} & \delta_{33} \end{bmatrix} = \begin{bmatrix} 1 & 0 & 0 \\ 0 & 1 & 0 \\ 0 & 0 & 1 \end{bmatrix} \tag{9.5}$$

The following relations are useful:

(1) $\delta_{ij} = 3$ (9.6)
(2) $\delta_{im} T_{mj} = T_{ij}$ (9.7)
(3) For the mutually perpendicular unit vectors $\mathbf{e}_1$, $\mathbf{e}_2$ and $\mathbf{e}_3$,

$$\mathbf{e}_i \mathbf{e}_j = \delta_{ij} \tag{9.8}$$

Permutation symbol

The permutation symbol is defined as

$$\varepsilon_{ijk} = \begin{cases} 1 & \text{if } ijk \text{ is even permutation of 1, 2, 3} \\ -1 & \text{if } ijk \text{ is odd permutation of 1, 2, 3} \\ 0 & \text{otherwise (i.e. if two of the indices are equal)} \end{cases} \tag{9.9}$$

where the even and odd permutations are indicated as

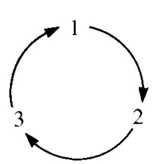

Even permutation

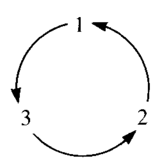

Odd permutation

The following relations are also used in this chapter:

(1) For the two vectors $\mathbf{a} = a_i\mathbf{e}_i$, and $\mathbf{b} = b_j\mathbf{e}_j$, then

$$\mathbf{a} \times \mathbf{b} = \varepsilon_{ijk} a_i b_j \mathbf{e}_k \tag{9.10}$$

where the unit vector $\mathbf{e}_k$ is normal to the plane containing both $\mathbf{e}_i$ and $\mathbf{e}_j$.

(2) For the matrix $\mathbf{m} = [m_{ij}]$, its determinant is

$$\det(\mathbf{m}) = \begin{vmatrix} m_{11} & m_{12} & m_{13} \\ m_{21} & m_{22} & m_{23} \\ m_{31} & m_{32} & m_{33} \end{vmatrix} = \tfrac{1}{6}\varepsilon_{ijk}\varepsilon_{pqr} m_{ip} m_{jq} m_{kr} \tag{9.11}$$

9.2.2 *Lagrangian and Eulerian descriptions*

Both the Lagrangian and Eulerian descriptions have been used in finite elasticity. The description of the relation between the undeformed and deformed configurations of a continuum can be considered as a 'mapping' between domains D_o and D (Fig. 9.3). To find the transformation relation, let X and x be two fixed rectangular Cartesian coordinates associated with the original and deformed configurations, respectively. The position of a generic particle P inside the domain D_o is defined by the position vector $\mathbf{X}$ and coordinates X_j ($j = 1,2,3$). After deformation, this particle assumes the location P' with the new position vector $\mathbf{x}$ and coordinates x_i ($i = 1,2,3$). Then, the 'mapping' or the deformation of the con-

Fig. 9.3. The undeformed configuration D_o and the deformed configuration D of an elastic body. (After Luo and Chou 1990b.)

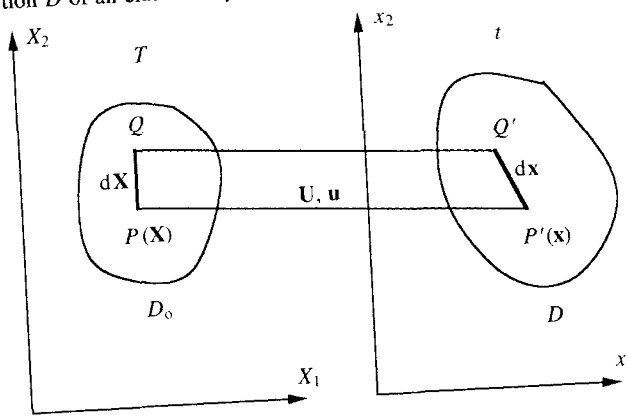

figuration can be described mathematically by the coordinate transformation between X_j and x_i.

The coordinate system X_1–X_2–X_3 is chosen as the reference system. The description of deformation, of which the independent variable is the particle position vector **X** in the original state, is known as the Lagrangian description. The reference system X is known as a Lagrangian coordinate. The transformation equation in terms of X_j is

$$x_i = x_i(X_1, X_2, X_3) \tag{9.12}$$

where the specified function x_i (X_1, X_2, X_3) is assumed to be continuous and differentiable. It follows, then:

$$\mathrm{d}x_i = \frac{\partial x_i}{\partial X_j}\,\mathrm{d}X_j \equiv x_{i,j}\,\mathrm{d}X_j \tag{9.13}$$

where the dummy, or repeating, index, j, denotes a summation over its range. The matrix form of Eq. (9.13) can be written as $[\mathrm{d}x] = [g][\mathrm{d}X]$, where the deformation gradient matrix $[g]$ is

$$g_{ij} = \frac{\partial x_i}{\partial X_j} \tag{9.14}$$

The strain tensor associated with the Lagrangian system is called the *Lagrangian strain* (E_{ij}), also known as the *Green's* or *St. Venant's strain*, and it is defined in matrix form as

$$[E] = \tfrac{1}{2}([g]^{\mathrm{T}} - [g] - [\delta]) \tag{9.15}$$

where $[g]^{\mathrm{T}}$ is the transpose of the deformation gradient matrix $[g]$, and $[\delta]$ is the Kronecker delta. The explicit form of Eq. (9.15) is given by

$$\begin{aligned}
E_{11} &= \frac{1}{2}\left(\frac{\partial x_1}{\partial X_1}\frac{\partial x_1}{\partial X_1} + \frac{\partial x_2}{\partial X_1}\frac{\partial x_2}{\partial X_1} - 1\right) \\
E_{22} &= \frac{1}{2}\left(\frac{\partial x_1}{\partial X_2}\frac{\partial x_1}{\partial X_2} + \frac{\partial x_2}{\partial X_2}\frac{\partial x_2}{\partial X_2} - 1\right) \\
E_{12} = E_{21} &= \frac{1}{2}\left(\frac{\partial x_1}{\partial X_1}\frac{\partial x_1}{\partial X_2} + \frac{\partial x_2}{\partial X_1}\frac{\partial x_2}{\partial X_2}\right)
\end{aligned} \tag{9.16}$$

On the other hand, the coordinate system x_1–x_2–x_3 can be chosen as the reference system. Then the description, in which the independent variable is the particle position vector **x** in the deformed state, is known as the *Eulerian description*, and the reference system x is known as an *Eulerian coordinate*. The transformation equation in terms of x_i is $X_i = X_i\ (x_1, x_2, x_3)$. Then,

$$[\mathrm{d}X] = [g]^{-1}[\mathrm{d}x] \tag{9.17}$$

where $[g]^{-1}$ is the inverse matrix of $[g]$ with the components

$$g_{ji}^{-1} = \frac{\partial X_j}{\partial x_i} = \frac{[\mathrm{co}(g_{ij})]^{\mathrm{T}}}{\det \mathbf{g}} \tag{9.18}$$

where $[\mathrm{co}(g_{ij})]^{\mathrm{T}}$ is the transpose of the cofactor matrix of g_{ij}, and $\det \mathbf{g}$ is the determinant of $[g]$.

The strain tensor associated with the Eulerian system (in terms of the deformed configuration) is termed the *Eulerian strain* (e_{ij}), which is also known as *Almansi's strain* for large deformation and *Cauchy's strain* for infinitesimal deformation (Fung 1977). It is defined as

$$[e] = \tfrac{1}{2}\{[\delta] - ([g]^{-1})^{\mathrm{T}} \cdot ([g]^{-1})\} \tag{9.19}$$

or

$$\begin{aligned}
2e_{11} &= 1 - \left(\frac{\partial X_1}{\partial x_1}\frac{\partial X_1}{\partial x_1} + \frac{\partial X_2}{\partial x_1}\frac{\partial X_2}{\partial x_1}\right) \\
2e_{22} &= 1 - \left(\frac{\partial X_1}{\partial x_2}\frac{\partial X_1}{\partial x_2} + \frac{\partial X_2}{\partial x_2}\frac{\partial X_2}{\partial x_2}\right) \\
2e_{12} &= 2e_{21} = -\left(\frac{\partial X_1}{\partial x_1}\frac{\partial X_1}{\partial x_2} + \frac{\partial X_2}{\partial x_1}\frac{\partial X_2}{\partial x_2}\right)
\end{aligned} \tag{9.20}$$

Equations (9.16) and (9.20) can be rewritten in terms of the displacement vectors $\mathbf{U}$ and $\mathbf{u}$, which are associated with the coordinate systems X and x (Fig. 9.3), respectively, and can be expressed as

$$\mathbf{U} = \mathbf{u} = \mathbf{x} - \mathbf{X} \tag{9.21}$$

Then, the alternate formulas for Lagrangian and Eulerian strain tensors are

$$E_{ij} = \frac{1}{2}\left(\frac{\partial U_i}{\partial X_j} + \frac{\partial U_j}{\partial X_i} + \frac{\partial U_k}{\partial X_i}\frac{\partial U_k}{\partial X_j}\right) \tag{9.22}$$

and

$$e_{ij} = \frac{1}{2}\left(\frac{\partial u_i}{\partial x_j} + \frac{\partial u_j}{\partial x_i} - \frac{\partial u_k}{\partial x_i}\frac{\partial u_k}{\partial x_j}\right) \tag{9.23}$$

If the displacement gradients are sufficiently small, the quadratic terms in Eqs. (9.22) and (9.23) can be neglected in comparison with the linear terms. Then, the Lagrangian and Eulerian strain tensors are reduced to the linear forms, and both are equal to the strain (ε_{ij}) for infinitesimal deformation

$$\varepsilon_{ij} = \frac{1}{2}\left(\frac{\partial u_i}{\partial x_j} + \frac{\partial u_j}{\partial x_i}\right) \tag{9.24}$$

The force acting per unit area is known as *stress*. In the case of finite deformation, the area and normal direction of a surface of an undeformed element may be quite different from those of the same surface in the deformed state. Thus, the stress can be defined by the force per either undeformed or deformed area; the former is known as the *Piola–Kirchhoff stress* or *Lagrangian stress* (Π_{ij}), and the latter is known as the *Cauchy's stress* or *Eulerian stress* (σ_{ij}).

For the purpose of illustration, consider a rectangular element $ABCD$ of unit thickness, which is deformed into $A'B'C'D'$ under a uniaxial load P (Fig. 9.4), and neglect the dimensional change in the thickness direction. The Eulerian stress is defined as the force per unit deformed area,

$$\sigma_{xx} = \frac{P}{C'D'} \tag{9.25}$$

The Lagrangian stress is defined as the force, which is acting on the deformed surface, divided by the original surface area (correspond-

Fig. 9.4. A force P acting on a deformable body.

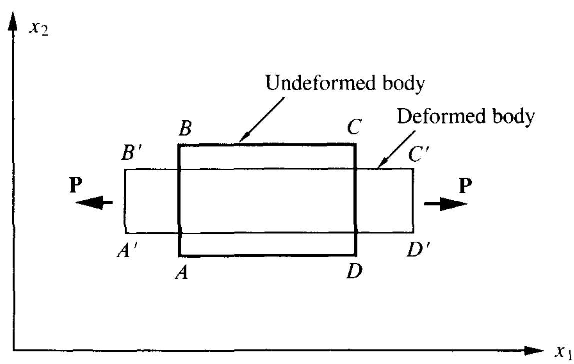

ing to the deformed area),

$$\Pi_{xx} = \frac{P}{CD} \tag{9.26}$$

From Eqs. (9.25) and (9.26),

$$\sigma_{xx} C'D' = \Pi_{xx} CD = P \tag{9.27}$$

The general relations between the two stress descriptions can be found by analyzing the deformation of a generic two-dimensional element as shown in Fig. 9.5. Let QR, with area δA and normal $\mathbf{N}$, be the edge surface of the element OQR in the undeformed state. The corresponding edge surface in the deformed state is $Q'R'$ with area δa and normal $\mathbf{n}$. The coordinates x_1–x_2 are fixed on the deformed element. Also let the surface force vector per unit area of the deformed surface ($Q'R'$) be $\mathbf{f}$ (traction), then the total surface force acting on $Q'R'$ is $\mathbf{f}\delta a$. The nominal traction, $\mathbf{F}$, acting on the undeformed edge surface (QR) is so defined that

$$\mathbf{F}\delta A = \mathbf{f}\delta a = \mathbf{P} \tag{9.28}$$

Fig. 9.5. The correspondence between Lagrangian stress and Eulerian stress.

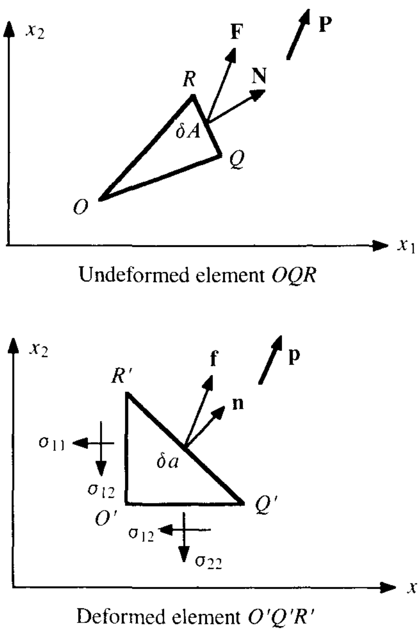

where $\mathbf{P}$ is the actual force acting on the surface element $Q'R'$ in the deformed state. By neglecting the body force and assuming that the displacement rate with respect to time is very small, the following relation from force equilibrium can be obtained:

$$f_i = \sigma_{ji} n_j \tag{9.29}$$

where f_i and n_j denote the components of $\mathbf{f}$ and $\mathbf{n}$, respectively. Similarly,

$$F_i = \Pi_{ji} N_j \tag{9.30}$$

where F_i and N_j denote the components of $\mathbf{F}$ and $\mathbf{N}$, respectively.

Substituting Eqs. (9.29) and (9.30) into Eq. (9.28) and applying the relation

$$N_i = (\det \mathbf{g})^{-1} n_j \frac{\delta a}{\delta A} g_{ji} \tag{9.31}$$

the result is

$$\sigma = (\det \mathbf{g})^{-1} \mathbf{g} \Pi \tag{9.32}$$

or

$$\sigma_{ji} = (\det \mathbf{g})^{-1} g_{jk} \Pi_{ki} \tag{9.33}$$

where $\det \mathbf{g}$ is the determinant of $\mathbf{g}$. The inversion of Eq. (9.32) gives

$$\Pi = (\det \mathbf{g}) \mathbf{g}^{-1} \sigma \tag{9.34}$$

or

$$\Pi_{ji} = (\det \mathbf{g}) g_{jk}^{-1} \sigma_{ki} \tag{9.35}$$

Note that the Eulerian stress tensor is symmetric (i.e. $\sigma_{ij} = \sigma_{ji}$) whereas the Lagrangian stress tensor (Eq. (9.34)) is not symmetric. However, the following quantity

$$P_{AB} = \frac{\partial X_A}{\partial x_i} \Pi_{Bi} = (\det \mathbf{g}) g_{Ai}^{-1} g_{Bj}^{-1} \sigma_{ji} \tag{9.36}$$

is symmetric, and P_{AB} is known as the *second Piola–Kirchhoff stress tensor*, or simply the *Kirchhoff stress*.

9.3 Constitutive relations based on the Lagrangian description

9.3.1 *Finite deformation of a composite lamina*

A basic element in a flexible composite is assumed to be a thin lamina consisting of straight, parallel continuous elastic fibers embedded in an elastic matrix which can sustain large deformation. It is also assumed that the lamina is homogeneous on a scale much larger than that of the inter-fiber spacing. Then, the flexible composite lamina can be treated as a homogeneous two-dimensional orthotropic elastic continuum. In this section, the constitutive equations for such an element under finite deformation are derived based on the Lagrangian description.

Figure 9.2(a) illustrates a unidirectional flexible composite lamina under a finite deformation, where the initial fiber orientation is at an angle θ_o with respect to the X_1 axis. The rectangular Cartesian coordinates l–t are along the initial fiber and transverse directions, respectively. Under loading, the rectangular element $ABCD$ in the undeformed lamina is deformed into a quadrilateral element $A'B'C'D'$ in the deformed lamina. There is an angle $\Delta\theta$ between AD and $A'D'$. Corresponding to this change, the current fiber orientation l' is at an angle θ with respect to the X_1 axis, and

$$\theta = \theta_o + \Delta\theta \tag{9.37}$$

Because of the low shear modulus of the matrix and the highly anisotropic nature ($E_{11} \gg E_{22}$) of flexible composites, $\Delta\theta$ may be quite large and the effective elastic properties of the composite become very sensitive to the fiber orientation. The geometric nonlinearity of a flexible composite is mainly caused by the reorientation of fibers. The material nonlinearity is also pronounced in elastomeric composites under large deformation.

The deformation of the basic element $ABCD$ (Fig. 9.2a) is further examined in Fig. 9.6. Let the rectangular Cartesian coordin-

Fig. 9.6. Deformation of a rectangular element of a composite lamina, referring to the principal material coordinate system. (After Luo and Chou 1990b.)

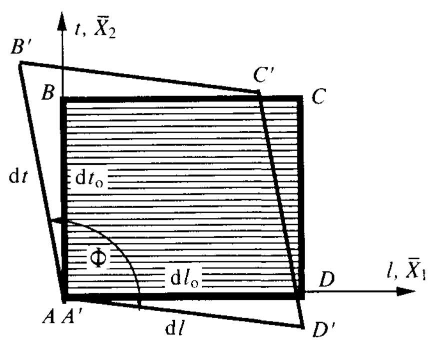

ate system $\bar{X}$ coincide with the initial principal material coordinates l–t, where the axis $\bar{X}_1$ is parallel to l. Here, a quantity with an over bar refers to the initial principal material coordinates. Then, the Lagrangian strain matrix in the system $\bar{X}$ is written as

$$[\bar{E}] = \tfrac{1}{2}([\bar{g}]^{\mathrm{T}}[\bar{g}] - [\delta]) \tag{9.38}$$

The deformation of the element shown in Fig. 9.6 can be expressed in terms of these Lagrangian strain components. Let the line elements $AD = dl_o$ and $AB = dt_o$ in the undeformed lamina; also $A'D' = dl$ and $A'B' = dt$ in the deformed lamina. Then, the following relations can be found:

$$\begin{aligned} 2\bar{E}_{11} &= [(\mathrm{d}l)^2 - (\mathrm{d}l_o)^2]/(\mathrm{d}l_o)^2 \\ 2\bar{E}_{22} &= [(\mathrm{d}t)^2 - (\mathrm{d}t_o)^2]/(\mathrm{d}t_o)^2 \\ 2\bar{E}_{12} &= -\sin(\Delta\phi)\sqrt{(1 + 2\bar{E}_{11})}\sqrt{(1 + 2\bar{E}_{22})} \end{aligned} \tag{9.39}$$

where

$$\Delta\phi = \angle B'A'D' - \angle BAD = \phi - \pi/2 \tag{9.40}$$

9.3.2 *Constitutive equations for a composite lamina*

9.3.2.1 *Strain-energy function*

Rivlin (1959) made the following remarks concerning the strain-energy function: 'It was realized that the physical properties of an elastic material can be characterized by a strain-energy function and that this cannot depend on the nine displacement gradients in a completely arbitrary fashion. And also if the material has symmetry, the dependence of the strain-energy on these strain components cannot be arbitrary either.' Following R. S. Rivlin (private communications, 1986–7), the strain-energy density treated here is assumed to be a function of the Lagrangian strain components referring to the principal material coordinates. In the two-dimensional case, referring to Eq. (9.39), the strain-energy per unit volume is written as

$$W = W(\bar{E}_{11}, \bar{E}_{22}, \bar{E}_{12}) \tag{9.41}$$

Since W is unchanged by the following permutation, namely,

$$\bar{X}_1 \to -\bar{X}_1 \quad \text{and} \quad \bar{x}_1 \to -\bar{x}_1$$

or

$$\bar{X}_2 \to -\bar{X}_2 \quad \text{and} \quad \bar{x}_2 \to -\bar{x}_2 \tag{9.42}$$

the strain-energy function must be an even function of $\bar{E}_{12}$. Then, Eq. (9.41) is rewritten as

$$W = W(\bar{E}_{11}, \bar{E}_{22}, \bar{E}_{12}^2) \tag{9.43}$$

Finally, the strain-energy per unit volume of the undeformed lamina is assumed in the following fourth-order polynomial form:

$$\begin{aligned} W = {} & \tfrac{1}{2}C_{11}\bar{E}_1^2 + \tfrac{1}{3}C_{111}\bar{E}_1^3 + \tfrac{1}{4}C_{1111}\bar{E}_1^4 + C_{12}\bar{E}_1\bar{E}_2 \\ & + \tfrac{1}{2}C_{22}\bar{E}_2^2 + \tfrac{1}{3}C_{222}\bar{E}_2^3 + \tfrac{1}{4}C_{2222}\bar{E}_2^4 + \tfrac{1}{2}C_{66}\bar{E}_6^2 + \tfrac{1}{4}C_{6666}\bar{E}_6^4 \end{aligned} \tag{9.44}$$

where C_{ij}, C_{ijk}, and C_{ijkl} are elastic constants. The short-hand notations are used, namely, $\bar{E}_1 = \bar{E}_{11}$, $\bar{E}_2 = \bar{E}_{22}$, and $\bar{E}_6 = 2\bar{E}_{12}$.

9.3.2.2 *General constitutive equations for a unidirectional lamina*

The stress matrix referring to the material principal coordinate system $\bar{X}_1$–$\bar{X}_2$, is given in terms of W (Rivlin 1970),

$$\begin{aligned} \bar{\Pi}_{ij} &= \frac{\partial W}{\partial \bar{g}_{ji}} \\ \bar{\sigma}_{ij} &= \frac{1}{\det \bar{\mathbf{g}}} \bar{g}_{ip} \frac{\partial W}{\partial \bar{g}_{jp}} \end{aligned} \tag{9.45}$$

Using Eqs. (9.38) and (9.43), it follows that

$$\begin{aligned} \bar{\Pi}_{ji} &= \frac{1}{2}\bar{g}_{ip}\left(\frac{\partial W}{\partial \bar{E}_{jp}} + \frac{\partial W}{\partial \bar{E}_{pj}}\right) \\ \bar{\sigma}_{ij} &= \frac{1}{\det \bar{\mathbf{g}}}\{W_{11}\bar{g}_{i1}\bar{g}_{j1} + W_{22}\bar{g}_{i2}\bar{g}_{j2} \\ &\qquad + \tfrac{1}{2}W_{12}(\bar{g}_{i1}\bar{g}_{j2} + \bar{g}_{i2}\bar{g}_{j1})\} \end{aligned} \tag{9.46}$$

where

$$\begin{aligned} W_{11} &= \frac{\partial W}{\partial \bar{E}_{11}} = C_{11}\bar{E}_{11} + C_{111}\bar{E}_{11}^2 + C_{1111}\bar{E}_{11}^3 + C_{12}\bar{E}_{22} \\ W_{22} &= \frac{\partial W}{\partial \bar{E}_{22}} = C_{22}\bar{E}_{22} + C_{222}\bar{E}_{22}^2 + C_{2222}\bar{E}_{22}^3 + C_{12}\bar{E}_{11} \\ W_{12} &= \frac{\partial W}{\partial \bar{E}_{12}} = 4(C_{66}\bar{E}_{12} + 4C_{6666}\bar{E}_{12}^3) \end{aligned} \tag{9.47}$$

To derive the general constitutive equations with reference axes other than the principal material directions, a two-dimensional rectangular Cartesian coordinate system X_1–X_2 is chosen in the plane of the lamina. The angle between X_i and $\bar{X}_i$ is θ_o (Fig. 9.7). Let $[a]$ be an orthogonal transformation matrix,

$$[a]=\begin{bmatrix}\cos\theta_o & -\sin\theta_o\\ \sin\theta_o & \cos\theta_o\end{bmatrix} \tag{9.48}$$

and $[X]=[a]\cdot[\bar{X}]$. Then, the transformation relations for the deformation gradient and Lagrangian strain between coordinate systems X and $\bar{X}$ are:

$$[\bar{g}]=[a]^{\mathrm{T}}[g][a] \tag{9.49}$$

and

$$[\bar{E}]=[a]^{\mathrm{T}}[E][a] \tag{9.50}$$

With Eq. (9.48), Eq. (9.50) yields

$$\begin{aligned}\bar{E}_{11}&=\tfrac{1}{2}E_{11}(1+\cos 2\theta_o)+E_{12}\sin 2\theta_o+\tfrac{1}{2}E_{22}(1-\cos 2\theta_o)\\ \bar{E}_{22}&=\tfrac{1}{2}E_{11}(1-\cos 2\theta_o)-E_{12}\sin 2\theta_o+\tfrac{1}{2}E_{22}(1+\cos 2\theta_o)\\ \bar{E}_{12}&=\bar{E}_{21}=\tfrac{1}{2}(E_{22}-E_{11})\sin 2\theta_o+E_{12}\cos 2\theta_o\end{aligned} \tag{9.51}$$

The stress matrix referring to the coordinate system X is

$$\begin{aligned}[\sigma]&=[a][\bar{\sigma}][a]^{\mathrm{T}}\\ [\Pi]&=[a][\bar{\Pi}][a]^{\mathrm{T}}\end{aligned} \tag{9.52}$$

With Eqs. (9.46) and (9.49), Eqs. (9.52) are expressed as

$$\begin{aligned}\sigma_{ij}=\frac{1}{\det\mathbf{g}}g_{ip}g_{jq}\{&a_{p1}a_{q1}W_{11}+a_{p2}a_{q2}W_{22}\\ &+\tfrac{1}{2}(a_{p1}a_{q2}+a_{p2}a_{q1})W_{12}\}\end{aligned} \tag{9.53}$$

and

$$\Pi_{ji}=g_{ip}\{a_{p1}a_{j1}W_{11}+a_{p2}a_{j2}W_{22}+\tfrac{1}{2}(a_{p1}a_{j2}+a_{p2}a_{j1})W_{12}\} \tag{9.54}$$

Then, from Eq. (9.48), Eq. (9.54) is given in the following explicit form:

$$
\begin{aligned}
\Pi_{11} &= [g_{11}c^2 + g_{12}cs]W_{11} + [g_{11}s^2 - g_{12}cs]W_{22} \\
&\quad + [-g_{11}cs + \tfrac{1}{2}g_{12}(c^2 - s^2)]W_{12} \\
\Pi_{22} &= [g_{22}s^2 + g_{21}cs]W_{11} + [g_{22}c^2 - g_{21}cs]W_{22} \\
&\quad + [g_{22}cs + \tfrac{1}{2}g_{21}(c^2 - s^2)]W_{12} \\
\Pi_{12} &= [g_{22}cs + g_{21}c^2]W_{11} + [g_{21}s^2 - g_{22}cs]W_{22} \\
&\quad + [-g_{21}cs + \tfrac{1}{2}g_{22}(c^2 - s^2)]W_{12} \\
\Pi_{21} &= [g_{11}cs + g_{12}s^2]W_{11} + [g_{12}c^2 - g_{11}cs]W_{22} \\
&\quad + [g_{12}cs + \tfrac{1}{2}g_{11}(c^2 - s^2)]W_{12}
\end{aligned}
\tag{9.55}
$$

where $c = \cos\theta_o$ and $s = \sin\theta_o$.

Equations (9.55) are the general constitutive equations for a composite lamina under finite deformation, where the deformation gradients, g_{ij}, represent the geometric nonlinearity influenced by the configuration changes of the lamina. The nonlinear expressions of W_{ij} (Eqs. (9.47)) represent the material nonlinearity of the composites. If the deformation of the composite lamina is infinitesimal (i.e. $g_{ij} = \delta_{ij}$) and only the linear terms (i.e. C_{ij}) remain in the expression of W_{ij}, Eqs. (9.55) can be easily reduced to the familiar linear stress–strain equation used for rigid composites.

For a specific deformation, the deformation gradient matrix, $[g]$, is calculated from Eq. (9.14); the Lagrangian strain referring to the principal material coordinates, $[\bar{E}]$, is obtained from Eqs. (9.15) and (9.51); and W_{ij} are obtained by introducing $[\bar{E}]$ into Eqs. (9.47). Then, the corresponding Lagrangian stresses, $[\Pi]$, can be determined from Eqs. (9.55). In the following Sections 9.3.2.3–9.3.2.5, this procedure is illustrated by some specific examples.

9.3.2.3 *Pure homogeneous deformation*

Consider the rectangular lamina of Fig. 9.7; its edges are parallel to the axes of the coordinate system X. The lamina is subjected to a pure homogeneous deformation with principal extension ratios λ_1 and λ_2 defined along the axes of the coordinate system X. The deformation is described by

$$
\begin{aligned}
x_1 &= \lambda_1 X_1 \\
x_2 &= \lambda_2 X_2
\end{aligned}
\tag{9.56}
$$

Consequently, referring to Eqs. (9.14) and (9.15),

$$[g] = \begin{bmatrix} \lambda_1 & 0 \\ 0 & \lambda_2 \end{bmatrix} \tag{9.57}$$

and

$$2[E] = \begin{bmatrix} \lambda_1^2 - 1 & 0 \\ 0 & \lambda_2^2 - 1 \end{bmatrix} \tag{9.58}$$

From Eqs. (9.51) and (9.58), the following can be obtained:

$$\begin{aligned} \bar{E}_{11} &= \tfrac{1}{4}[(\lambda_1^2 + \lambda_2^2 - 2) + (\lambda_1^2 - \lambda_2^2)\cos 2\theta_o] \\ \bar{E}_{22} &= \tfrac{1}{4}[(\lambda_1^2 + \lambda_2^2 - 2) - (\lambda_1^2 - \lambda_2^2)\cos 2\theta_o] \\ \bar{E}_{12} &= \tfrac{1}{4}(\lambda_2^2 - \lambda_1^2)\sin 2\theta_o \end{aligned} \tag{9.59}$$

Then, the components of the Lagrangian stress are obtained from Eqs. (9.55) and (9.57) as

$$\begin{aligned} \Pi_{11} &= \lambda_1(c^2 W_{11} + s^2 W_{22} - csW_{12}) \\ \Pi_{22} &= \lambda_2(s^2 W_{11} + c^2 W_{22} + csW_{12}) \\ \Pi_{12} &= \lambda_2[cs(W_{11} - W_{22}) + \tfrac{1}{2}(c^2 - s^2)W_{12}] \\ \Pi_{21} &= \lambda_1[cs(W_{11} - W_{22}) + \tfrac{1}{2}(c^2 - s^2)W_{12}] \end{aligned} \tag{9.60}$$

where W_{11}, W_{22} and W_{12} are given by Eqs. (9.47) and (9.59).

Fig. 9.7. Pure homogeneous deformation. (After Luo and Chou 1990b.)

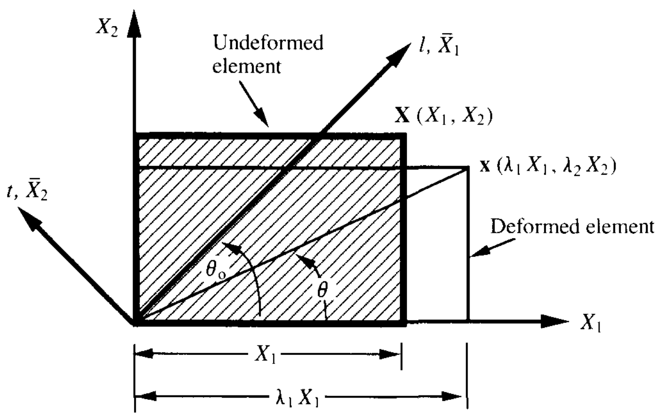

9.3.2.4 *Simple shear*

Suppose that the rectangular lamina, with its edges parallel to the axes of the coordinate system X, is subjected to a simple shear of amount K in the direction of the X_1 axis (Fig. 9.8). Then, the deformation is described by

$$\begin{aligned} x_1 &= X_1 + KX_2 \\ x_2 &= X_2 \end{aligned} \tag{9.61}$$

For this deformation, referring to Eqs. (9.14), (9.15) and (9.51),

$$[g] = \begin{bmatrix} 1 & K \\ 0 & 1 \end{bmatrix}, \qquad 2[E] = \begin{bmatrix} 0 & K \\ K & K^2 \end{bmatrix} \tag{9.62}$$

and

$$\begin{aligned} \bar{E}_{12} &= \tfrac{1}{4}[K^2 + (2K\sin 2\theta_o - K^2\cos 2\theta_o)] \\ \bar{E}_{22} &= \tfrac{1}{4}[K^2 - (2K\sin 2\theta_o - K^2\cos 2\theta_o)] \\ \bar{E}_{12} &= \tfrac{1}{4}[K^2\sin 2\theta_o + 2K\cos 2\theta_o] \end{aligned} \tag{9.63}$$

Then, the components of the Lagrangian stress are obtained from Eqs. (9.55) and (9.62):

$$\begin{aligned} \Pi_{11} &= [c^2 + Kcs]W_{11} + [s^2 - Kcs]W_{22} \\ &\quad + [-cs + \tfrac{1}{2}K(c^2 - s^2)]W_{12} \\ \Pi_{22} &= s^2W_{11} + c^2W_{22} + csW_{12} \\ \Pi_{12} &= csW_{11} - csW_{22} + \tfrac{1}{2}(c^2 - s^2)W_{12} \\ \Pi_{21} &= [cs + Ks^2]W_{11} + [Kc^2 - cs]W_{22} + [Kcs + \tfrac{1}{2}(c^2 - s^2)]W_{12} \end{aligned} \tag{9.64}$$

Fig. 9.8. Simple shear deformation. (After Luo and Chou 1990b.)

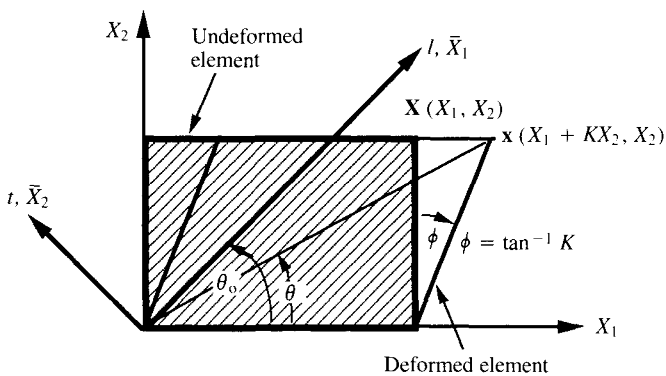

Considering the example of $\theta_o = 45°$, Eqs. (9.63) yield

$$\begin{aligned}\bar{E}_{11} &= \tfrac{1}{2}K + \tfrac{1}{4}K^2 \\ \bar{E}_{22} &= -\tfrac{1}{2}K + \tfrac{1}{4}K^2 \\ \bar{E}_{12} &= \tfrac{1}{4}K^2\end{aligned} \tag{9.65}$$

Then Eqs. (9.64) give

$$\begin{aligned}\Pi_{11} &= \tfrac{1}{2}\{(1+K)W_{11} + (1-K)W_{22} - W_{12}\} \\ \Pi_{22} &= \tfrac{1}{2}\{W_{11} + W_{22} + W_{12}\} \\ \Pi_{12} &= \tfrac{1}{2}\{W_{11} - W_{22}\} \\ \Pi_{21} &= \tfrac{1}{2}\{(1+K)W_{11} + (K-1)W_{22} + KW_{12}\}\end{aligned} \tag{9.66}$$

Figure 9.9 shows the theoretical prediction of the stress–strain relation (Eqs. (9.64)) for Kevlar/silicone elastomer laminae with various initial fiber orientations under simple shear deformation. The elastic constants used in the analysis are shown in Table 9.1 (Luo 1988). The result shows that the simple shear properties of a composite lamina under finite deformation are significantly influenced by the fiber orientation. Figure 9.10 gives the comparison between analytical predictions and experimental results of a 0° specimen under simple shear. Figure 9.11 shows the same comparison on a

Fig. 9.9. Theoretical predictions of simple shear deformation of Kevlar/silicone elastomer composite laminae for various initial fiber orientations. (After Luo and Chou 1990b.)

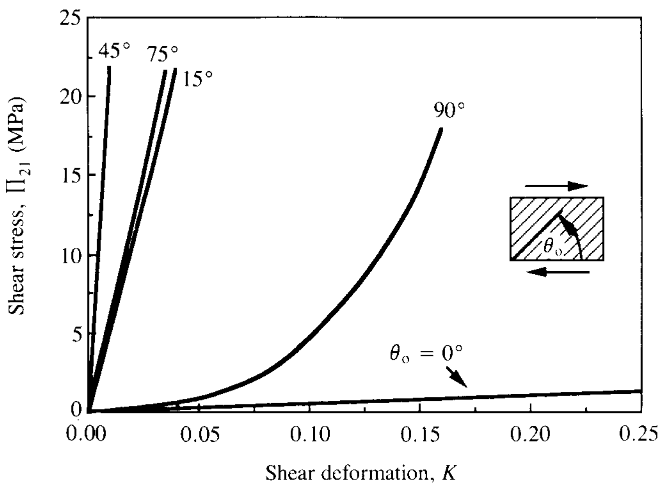

Table 9.1. *Elastic constants of Kevlar-49/silicone flexible composites (After Luo, 1988).*

S_{11}	$(\mathrm{MPa})^{-1}$	0.114×10^{-3}
S_{1111}	$(\mathrm{MPa})^{-3}$	0
S_{12}	$(\mathrm{MPa})^{-1}$	-69.9×10^{-6}
S_{22}	$(\mathrm{MPa})^{-1}$	0.306
S_{2222}	$(\mathrm{MPa})^{-3}$	0.563
S_{66}	$(\mathrm{MPa})^{-1}$	0.387
S_{6666}	$(\mathrm{MPa})^{-3}$	77.5×10^{-3}
S_{166}	$(\mathrm{MPa})^{-2}$	3.43×10^{-6}
S_{2266}	$(\mathrm{MPa})^{-3}$	56.3×10^{-3}
C_{11}	(MPa)	8.6×10^{3}
C_{1111}	(MPa)	0
C_{12}	(MPa)	-1.3
C_{22}	(MPa)	2.77
C_{2222}	(MPa)	-12.5
C_{66}	(MPa)	2.55
C_{6666}	(MPa)	-2.45

Fig. 9.10. Comparisons between theoretical predictions and experimental data of simple shear response of 0° Kevlar/silicone elastomer composite laminae. (After Luo and Chou 1990b.)

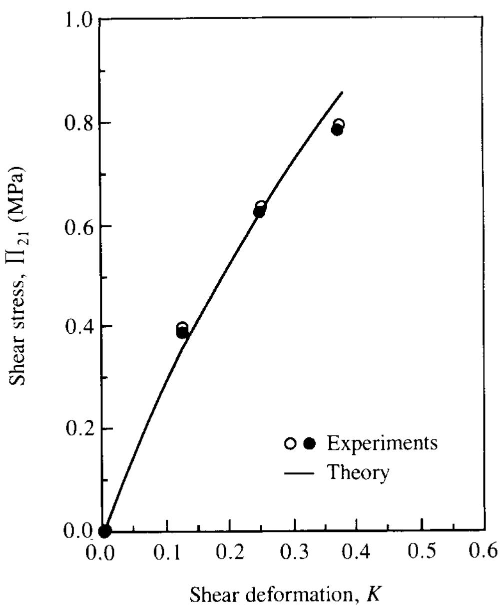

90° specimen; the experimental data, which are obtained from three-rail shear tests (Whitney, Daniel and Pipes 1982), are lower than the predicted values at large shear deformation. This is caused by the edge effects, and fiber pull-out from clamped edges for 90° specimens at large deformation.

9.3.2.5 *Simple shear superposed on simple extension*

A rectangular lamina, with the edges parallel to the axes of the rectangular Cartesian coordinate system X, is first subjected to the pure homogeneous deformation described by Eqs. (9.56), followed by a simple shear of magnitude K. There are two cases for the direction of the shear deformation: (1) parallel to the X_1 axis, and (2) parallel to the X_2 axis; both are discussed in the following:

Case 1

Figure 9.12(a) illustrates this deformation, which can be specified as

$$\begin{aligned} x_1 &= \lambda_1 X_1 + K\lambda_2 X_2 \\ x_2 &= \lambda_2 X_2 \end{aligned} \tag{9.67}$$

Fig. 9.11. Comparisons between theoretical predictions and experimental data of simple shear response of 90° Kevlar/silicone elastomer composite lamina. (After Luo and Chou 1990b.)

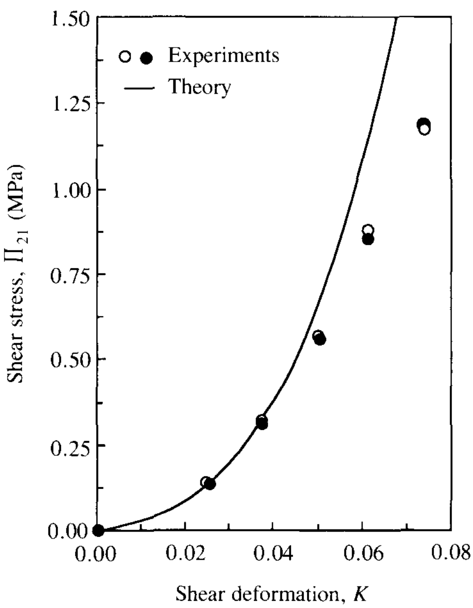

From Eqs. (9.14), (9.15) and (9.51),

$$[g]=\begin{bmatrix}\lambda_1 & K\lambda_2\\ 0 & \lambda_2\end{bmatrix},\qquad 2[E]=\begin{bmatrix}\lambda_1^2-1 & K\lambda_1\lambda_2\\ K\lambda_1\lambda_2 & \lambda_2^2(K^2+1)-1\end{bmatrix} \tag{9.68}$$

and

$$\begin{aligned}\bar{E}_{11}&=\tfrac{1}{4}[(\lambda_1^2+\lambda_2^2-2+\lambda_2^2K^2)+(\lambda_1^2-\lambda_2^2-\lambda_2^2K^2)\cos 2\theta_o\\&\quad+2K\lambda_1\lambda_2\sin 2\theta_o]\\ \bar{E}_{22}&=\tfrac{1}{4}[(\lambda_1^2+\lambda_2^2-2+\lambda_2^2K^2)-(\lambda_1^2-\lambda_2^2-\lambda_2^2K^2)\cos 2\theta_o\\&\quad-2K\lambda_1\lambda_2\sin 2\theta_o]\\ \bar{E}_{12}&=\tfrac{1}{4}[(\lambda_2^2-\lambda_1^2+\lambda_2^2K^2)\sin 2\theta_o+2K\lambda_1\lambda_2\cos 2\theta_o]\end{aligned}\tag{9.69}$$

The components of the Lagrangian stress are obtained from Eqs.

Fig. 9.12. Simple shear superposed on simple extension. (After Luo and Chou 1990b.)

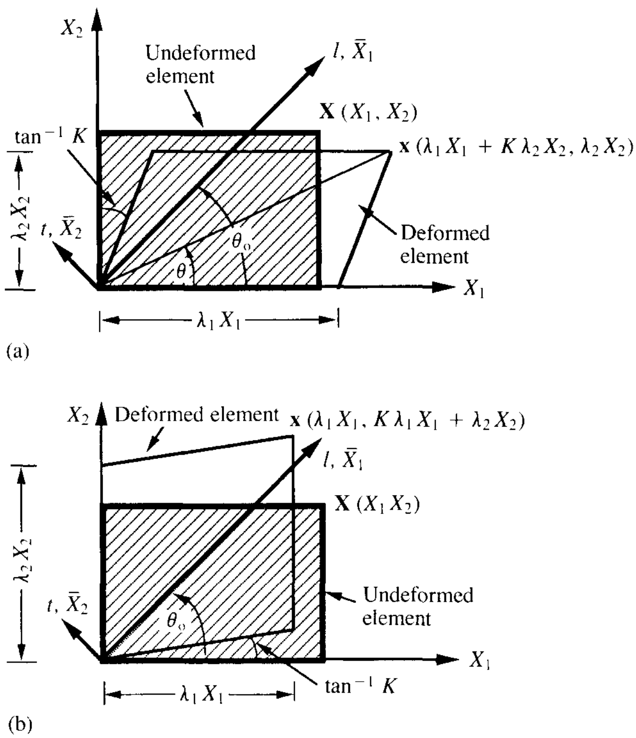

(9.55) and (9.68):

$$\begin{aligned}\Pi_{11} &= [\lambda_1 c^2 + K\lambda_2 cs]W_{11} + [\lambda_1 s^2 - K\lambda_2 cs]W_{22} \\ &\quad + [-\lambda_1 cs + \tfrac{1}{2}K\lambda_2(c^2 - s^2)]W_{12} \\ \Pi_{22} &= \lambda_2[s^2 W_{11} + c^2 W_{22} + csW_{12}] \\ \Pi_{12} &= \lambda_2[csW_{11} - csW_{22} + \tfrac{1}{2}(c^2 - s^2)W_{12}] \\ \Pi_{21} &= [\lambda_1 cs + K\lambda_2 s^2]W_{11} + [K\lambda_2 c^2 - \lambda_1 cs]W_{22} \\ &\quad + [K\lambda_2 cs + \tfrac{1}{2}\lambda_1(c^2 - s^2)]W_{12}\end{aligned} \tag{9.70}$$

Case 2

Figure 9.12(b) shows the deformation defined by

$$\begin{aligned}x_1 &= \lambda_1 X_1 \\ x_2 &= K\lambda_1 X_1 + \lambda_2 X_2\end{aligned} \tag{9.71}$$

For this deformation, referring to Eqs. (9.14), (9.15) and (9.51),

$$[g] = \begin{bmatrix} \lambda_1 & 0 \\ K\lambda_1 & \lambda_2 \end{bmatrix}, \qquad 2[E] = \begin{bmatrix} \lambda_1^2(K^2+1) - 1 & K\lambda_1\lambda_2 \\ K\lambda_1\lambda_2 & \lambda_2^2 - 1 \end{bmatrix} \tag{9.72}$$

and

$$\begin{aligned}\bar{E}_{11} &= \tfrac{1}{4}[(\lambda_1^2 + \lambda_2^2 - 2 + \lambda_1^2 K^2) + (\lambda_1^2 - \lambda_2^2 + \lambda_1^2 K^2)\cos 2\theta_o \\ &\quad + 2K\lambda_1\lambda_2 \sin 2\theta_o] \\ \bar{E}_{22} &= \tfrac{1}{4}[(\lambda_1^2 + \lambda_2^2 - 2 + \lambda_1^2 K^2) - (\lambda_1^2 - \lambda_2^2 + \lambda_1^2 K^2)\cos 2\theta_o \\ &\quad - 2K\lambda_1\lambda_2 \sin 2\theta_o] \\ \bar{E}_{12} &= \tfrac{1}{4}[(\lambda_2^2 - \lambda_1^2 + \lambda_1^2 K^2)\sin 2\theta_o + 2K\lambda_1\lambda_2 \cos 2\theta_o]\end{aligned} \tag{9.73}$$

The components of the Lagrangian stress obtained from Eqs. (9.55) and (9.72) are:

$$\begin{aligned}\Pi_{11} &= \lambda_1[c^2 W_{11} + s^2 W_{22} - csW_{12}] \\ \Pi_{22} &= [\lambda_2 s^2 + K\lambda_1 cs]W_{11} + [\lambda_2 c^2 - K\lambda_1 cs]W_{22} \\ &\quad + [\lambda_2 cs + \tfrac{1}{2}K\lambda_1(c^2 - s^2)]W_{12} \\ \Pi_{12} &= [\lambda_2 cs + K\lambda_1 c^2]W_{11} + [K\lambda_1 s^2 - \lambda_2 cs]W_{22} \\ &\quad + [-K\lambda_1 cs + \tfrac{1}{2}\lambda_2(c^2 - s^2)]W_{12} \\ \Pi_{21} &= \lambda_1[csW_{11} - csW_{22} + \tfrac{1}{2}(c^2 - s^2)W_{12}]\end{aligned} \tag{9.74}$$

Figure 9.13 illustrates an off-axis specimen under uniaxial tension. It is understood that the clamping of the specimen at the ends induces a local non-uniform strain field. However, if the length-to-width ratio of the specimen is sufficiently large, a uniform state of stress and strain prevails at the center of the specimen (Pagano and Halpin 1968), and the central lines of the specimen remain straight in the X_1 direction. Then, this deformation corresponds to Case 1, namely, 'simple shear superposed on simple extension'. The uniaxial loading condition can be described as $\Pi_{11} \neq 0$, $\Pi_{22} = 0$ and $\Pi_{21} = 0$. Then, from Eqs. (9.74),

$$\begin{aligned} \Pi_{11} &= \lambda_1[c^2W_{11} + s^2W_{22} - csW_{12}] \\ 0 &= s^2W_{11} + c^2W_{22} + csW_{12} \\ 0 &= csW_{11} - csW_{22} + \tfrac{1}{2}(c^2 - s^2)W_{12} \end{aligned} \tag{9.75}$$

where W_{ij} are obtained by from Eqs. (9.68) and (9.47). The three unknowns λ_1, λ_2 and K in Eqs. (9.75) can be solved from these equations. Figure 9.14 shows the comparison between analytical predictions and experimental results for the off-axis response of Kevlar/silicone elastomer laminae under simple tension. The fiber initial orientations are 10°, 30° and 60°. The elastic constants used in the calculation are shown in Table 9.1.

Fig. 9.13. Off-axis specimens of flexible composite laminae (a) without loading, (b) with loading. The 15° one is tirecord/rubber, and the 10° and 30° ones are Kevlar/silicone elastomer. (After Luo and Chou 1988a.)

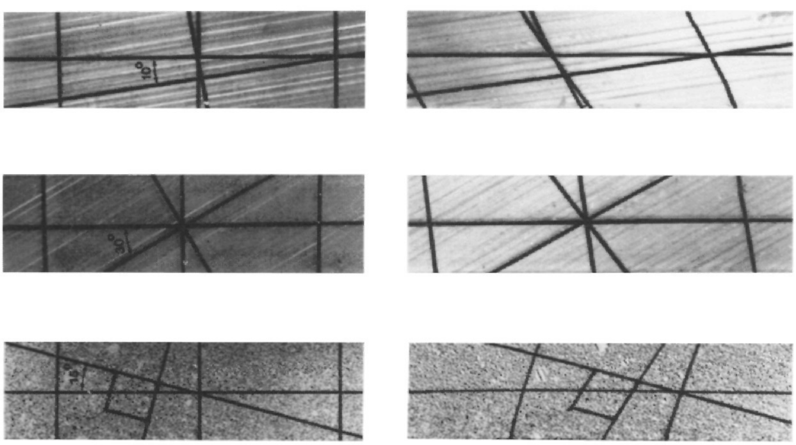

(a) (b)

9.3.3 Constitutive equations of flexible composite laminates

9.3.3.1 Constitutive equations

The analytical methodology developed in Section 9.3.2 for composite laminae is applied to study the constitutive relations of laminated flexible composites (Fig. 9.15) under finite plane deformation (Luo and Chou 1989). The stress resultant in Lagrangian description (N_{ij}) is defined as

$$N_{ij} = \int_{-h/2}^{h/2} \Pi_{ij}\, dz \tag{9.76}$$

where h is the initial laminate thickness. N_{ij} so defined gives the total force in the i direction per unit length of the undeformed laminate.

Assume that the laminate is composed of n layers of unidirectional laminae. By neglecting the interlaminar shear deformation, the deformation gradient, g_{ij} (Eq. (9.14)), has the same value for all the layers; this is also true for E_{ij} (Eq. (9.15)). For an arbitrary kth lamina within the laminate, let $\theta_0^{(k)}$ be the fiber orientation angle

Fig. 9.14. Comparisons between theoretical predictions and experimental results on 10°, 30° and 60° off-axis stress–strain response of Kevlar/silicone elastomer composite laminae.

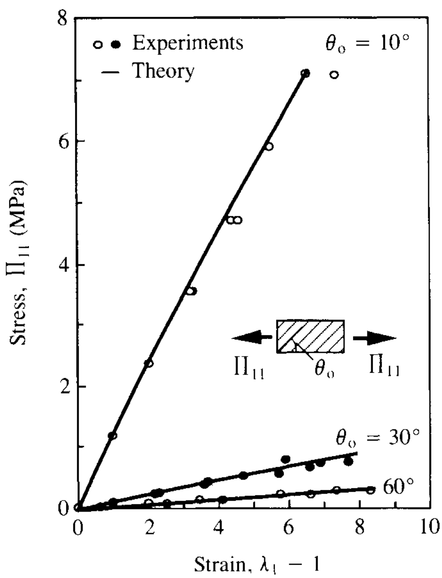

with respect to the coordinate X_1, and $a_{ij}^{(k)}$ the values given by Eq. (9.48) for $\theta_o = \theta_o^{(k)}$. Also, for the kth lamina, let $\bar{E}_{ij}^{(k)}$ be the values of $\bar{E}_{ij}$ given by Eqs. (9.51), and $W_{ij}^{(k)}$ the values of W_{ij} given by Eqs. (9.47). Then, from Eqs. (9.54) and (9.76) the following can be derived:

$$N_{ji} = g_{ip} \sum_{k=1}^{n} (h_k - h_{k-1})\{a_{p1}^{(k)}a_{j1}^{(k)}W_{11}^{(k)} + a_{p2}^{(k)}a_{j2}^{(k)}W_{22}^{(k)} + \tfrac{1}{2}(a_{p1}^{(k)}a_{j2}^{(k)} + a_{p2}^{(k)}a_{j1}^{(k)})W_{12}^{(k)}\} \tag{9.77a}$$

If the laminae are identical in thickness, t, then

$$N_{ji} = tg_{ip} \sum_{k=1}^{n} \{a_{p1}^{(k)}a_{j1}^{(k)}W_{11}^{(k)} + a_{p2}^{(k)}a_{j2}^{(k)}W_{22}^{(k)} + \tfrac{1}{2}(a_{p1}^{(k)}a_{j2}^{(k)} + a_{p2}^{(k)}a_{j1}^{(k)})W_{12}^{(k)}\} \tag{9.77b}$$

Equations (9.77) are the general constitutive equations for flexible composite laminates under finite deformations. The applications of the constitutive relations are exemplified in the following.

9.3.3.2 *Homogeneous deformation*

The homogeneous deformation of a composite laminate (Fig. 9.16) is defined by

$$\begin{aligned} x_1 &= \lambda_1 X_1 \\ x_2 &= \lambda_2 X_2 \end{aligned} \tag{9.78}$$

Fig. 9.15. A composite laminate. (After Luo and Chou 1989.)

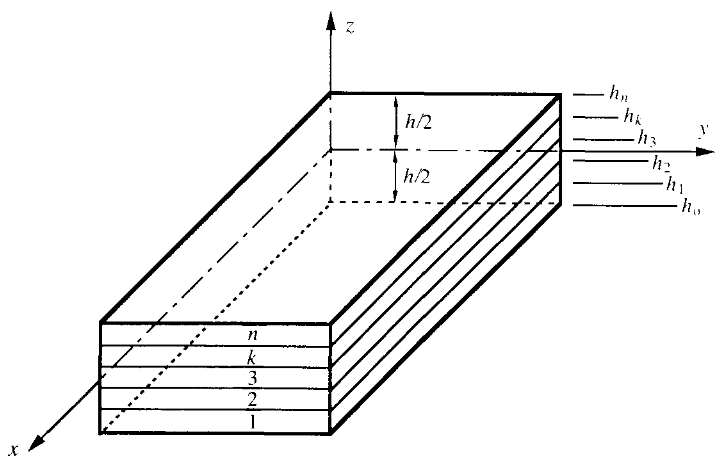

where λ_1 and λ_2 are the extension ratios in the X_1 and X_2 directions, respectively. Thus, referring to Eqs. (9.14) and (9.15), for all laminae:

$$[g] = \begin{bmatrix} \lambda_1 & 0 \\ 0 & \lambda_2 \end{bmatrix}, \qquad 2[E] = \begin{bmatrix} \lambda_1^2 - 1 & 0 \\ 0 & \lambda_2^2 - 1 \end{bmatrix} \tag{9.79}$$

The Lagrangian strains referring to the principal material coordinate for the kth lamina are obtained from Eqs. (9.51)

$$\begin{aligned} \bar{E}_{11}^{(k)} &= \tfrac{1}{2}(\lambda_1^2 \cos^2 \theta_o^{(k)} + \lambda_2^2 \sin^2 \theta_o^{(k)} - 1) \\ \bar{E}_{22}^{(k)} &= \tfrac{1}{2}(\lambda_1^2 \sin^2 \theta_o^{(k)} + \lambda_2^2 \cos^2 \theta_o^{(k)} - 1) \\ \bar{E}_{12}^{(k)} &= \tfrac{1}{2}(\lambda_2^2 - \lambda_1^2) \sin \theta_o^{(k)} \cos \theta_o^{(k)} \end{aligned} \tag{9.80}$$

Then, the components of the Lagrangian stress resultant are obtained from Eq. (9.77b)

$$\begin{aligned} N_{11} &= \frac{t}{2} \lambda_1 \sum_{k=1}^{n} \{W_{11}^{(k)}(1 + \cos 2\theta_o^{(k)}) \\ &\quad + W_{22}^{(k)}(1 - \cos 2\theta_o^{(k)}) - W_{12}^{(k)} \sin 2\theta_o^{(k)}\} \\ N_{22} &= \frac{t}{2} \lambda_2 \sum_{k=1}^{n} \{W_{11}^{(k)}(1 - \cos 2\theta_o^{(k)}) \\ &\quad + W_{22}^{(k)}(1 + \cos 2\theta_o^{(k)}) + W_{12}^{(k)} \sin 2\theta_o^{(k)}\} \\ N_{12} &= \frac{t}{2} \lambda_2 \sum_{k=1}^{n} \{(W_{11}^{(k)} - W_{22}^{(k)}) \sin 2\theta_o^{(k)} + W_{12}^{(k)} \cos 2\theta_o^{(k)}\} \\ N_{21} &= \frac{t}{2} \lambda_1 \sum_{k=1}^{n} \{(W_{11}^{(k)} - W_{22}^{(k)}) \sin 2\theta_o^{(k)} + W_{12}^{(k)} \cos 2\theta_o^{(k)}\} \end{aligned} \tag{9.81}$$

Fig. 9.16. A symmetric flexible composite laminate under a uniaxial load. (After Luo and Chou 1989.)

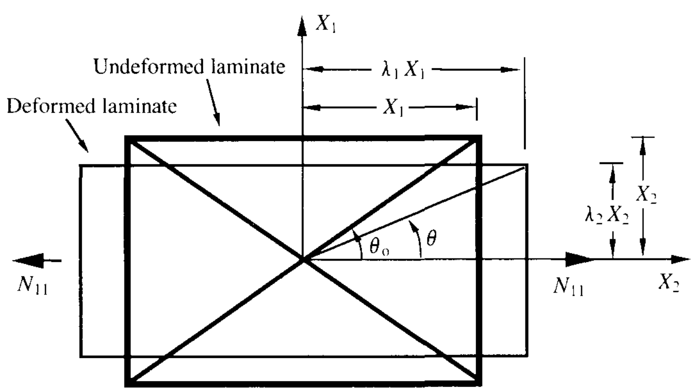

where $W_{11}^{(k)}$, $W_{22}^{(k)}$ and $W_{12}^{(k)}$ are obtained from Eqs. (9.47) and (9.80) with two variables λ_1 and λ_2.

9.3.3.3 *Simple extension of a symmetric composite laminate*

(A) Tensile stress–strain relation

The state of homogeneous deformation is assumed for a symmetric composite laminate with fiber orientation sequences of $+\theta_o/-\theta_o/-\theta_o/+\theta_o$ under unidirectional tension. Because $\bar{E}_{11}$ and $\bar{E}_{22}$ are even functions of θ_o, and $\bar{E}_{12}$ is an odd function of θ_o (Eqs. (9.80)), Eqs. (9.47) become

$$
\begin{aligned}
W_{11}^{(\theta)} &= W_{11}^{(-\theta)} \\
W_{22}^{(\theta)} &= W_{22}^{(-\theta)} \\
W_{12}^{(\theta)} &= -W_{12}^{(-\theta)}
\end{aligned}
\tag{9.82}
$$

Then, Eqs. (9.81) can be reduced to

$$
\begin{aligned}
N_{11} &= \frac{h}{2}\lambda_1\{W_{11}^{(\theta)}(1+\cos 2\theta_o) \\
&\quad + W_{22}^{(\theta)}(1-\cos 2\theta_o) - W_{12}^{(\theta)}\sin 2\theta_o\} \\
N_{22} &= \frac{h}{2}\lambda_2\{W_{11}^{(\theta)}(1-\cos 2\theta_o) \\
&\quad + W_{22}^{(\theta)}(1+\cos 2\theta_o) + W_{12}^{(\theta)}\sin 2\theta_o\} \\
N_{12} &= N_{21} = 0
\end{aligned}
\tag{9.83}
$$

where h is the thickness of the laminate; $W_{ij}^{(\theta)}$, obtained from Eqs. (9.47) and (9.80), is a function of λ_1 and λ_2. With the uniaxial loading condition and the values of elastic constants, the two unknowns, λ_1 and λ_2, in Eqs. (9.83) can be solved.

For example, let $\theta_o = 45°$, from Eqs. (9.47), (9.80) and (9.83),

$$
\begin{aligned}
N_{11}/h &= \lambda_1\{C_{66}(\lambda_1^2-\lambda_2^2) + \tfrac{1}{4}C_{6666}(\lambda_1^2-\lambda_2^2)^3\} \\
N_{22}/h &= 0 \\
&= (D-4C_{66})\lambda_1^2 - (D+4C_{66})\lambda_2^2 \\
&\quad + \tfrac{1}{4}(C_{111}+C_{222})(\lambda_1^2+\lambda_2^2-2)^2 \\
&\quad + \tfrac{1}{16}(C_{1111}+C_{2222})(\lambda_1^2+\lambda_2^2-2)^3 + C_{6666}(\lambda_2^2-\lambda_1^2)^3
\end{aligned}
\tag{9.84}
$$

where $D = C_{11} + 2C_{12} + C_{22}$.

Figure 9.17 shows the comparison between the theoretical predictions and experimental results of the stress–strain relation of $[\pm 45°]_s$ Kevlar/silicone elastomer composite laminates under uniaxial load. Reasonable agreement has been found.

(B) Effective Poisson's ratio

The Poisson's ratio is defined as the negative ratio of the strain in the X_j direction to the strain in the X_i direction due to an applied stress in the X_i direction. The Poisson's ratio of a symmetric composite laminate was derived by Posfalvi (1977) based upon a finite deformation consideration. Although experimental results of large deformation were presented, the comparison of theory with experiments was still limited to the small deformation range.

From the above analysis the effective Poisson's ratio in the finite deformation range can be readily predicted. For example, for a $[+\theta_o/-\theta_o]_s$ laminate under unidirectional load, the effective Poisson's ratio at a given strain level can be determined from Eqs. (9.79) as

$$\frac{E_{22}}{E_{11}}=\frac{\lambda_2^2-1}{\lambda_1^2-1} \tag{9.85}$$

Fig. 9.17. Comparisons between theoretical predictions and experimental data of stress–strain response of a $[\pm 45°]_s$ Kevlar/silicone elastomer composite laminate under uniaxial load. (After Luo and Chou 1989.)

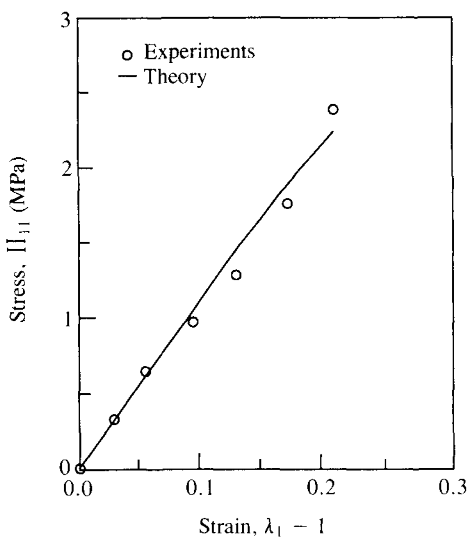

where the relation between λ_1 and λ_2 can be obtained from Eqs. (9.83) with $N_{22}=0$.

The approximate order of the ratio E_{22}/E_{11} can be obtained by neglecting the non-linear terms (i.e. $C_{111}, \ldots, C_{6666}$, etc.) in the expressions of Eqs. (9.47) for W_{ij}. Then

$$-\frac{\lambda_2^2-1}{\lambda_1^2-1}=\frac{A}{B} \tag{9.86}$$

where

$$\begin{aligned} A &= C_{11}\cos^2\theta_o\sin^2\theta_o + C_{12}(\sin^4\theta_o+\cos^4\theta_o) \\ &\quad + C_{22}\cos^2\theta_o\sin^2\theta_o - 4C_{66}\cos^2\theta_o\sin^2\theta_o \\ B &= C_{11}\sin^4\theta_o + 2C_{12}\cos^2\theta_o\sin^2\theta_o + C_{22}\cos^4\theta_o \\ &\quad + 4C_{66}\cos^2\theta_o\sin^2\theta_o \end{aligned}$$

For example, for $\theta_o = 45°$, Eq. (9.86) yields

$$\frac{A}{B}=\frac{(C_{11}+2C_{12}+C_{22})-4C_{66}}{(C_{11}+2C_{12}+C_{22})+4C_{66}} \tag{9.87}$$

Since the shear modulus C_{66} for flexible composites is relatively small, it can be assumed $A/B \approx 1$. Then, Eq. (9.85) becomes

$$\frac{E_{22}}{E_{11}}=-1 \tag{9.88}$$

Furthermore, if the flexible composite is very stiff in the fiber direction (i.e. $C_{11} \gg C_{ij}$, $ij \neq 11$) and $\theta_o \neq 0$, Eq. (9.86) becomes

$$\frac{E_{22}}{E_{11}}=\frac{\lambda_2^2-1}{\lambda_1^2-1}= -\frac{\cos^2\theta_o}{\sin^2\theta_o} \tag{9.89}$$

The results of Eq. (9.89) can also be derived by using the 'ideal fiber reinforced material theory' (Adkins and Rivlin 1955).

Figure 9.18 gives the comparison between theoretical predictions and experimental results of the ratio λ_2/λ_1 for $[\pm\theta_o]_s$ Kevlar/silicone elastomer composite laminates under uniaxial load. The initial fiber orientations are 15°, 30° and 45°. Very good agreement has been found.

Also, using the definition of Posfalvi (1977), the current Poisson's ratio at a given strain level can be derived from Eq. (9.86) as

$$\frac{d\lambda_2}{d\lambda_1}= -\frac{\lambda_1}{\lambda_2}\frac{A}{B} \tag{9.90}$$

Referring to Fig. 9.16, the current fiber orientation, $\theta^{(k)}$, of the kth lamina, can be expressed in terms of λ_1, λ_2 and the initial fiber orientation $\theta_o^{(k)}$ as

$$\tan\theta^{(k)} = \frac{\lambda_2 \sin\theta_o^{(k)}}{\lambda_1 \cos\theta_o^{(k)}} = \frac{\lambda_2}{\lambda_1}\tan\theta_o^{(k)} \tag{9.91}$$

where λ_1 and λ_2 are obtained by solving Eqs. (9.83).

9.3.4 *Determination of elastic constants*

In Section 9.3.2.1, the strain-energy per unit volume of an undeformed lamina is assumed in a polynomial form (Eq. (9.44)). The elastic constants in the strain-energy expression need to be determined experimentally. Some experimental methods for characterizing these constants are summarized below (Luo 1988).

9.3.4.1 *Tensile properties*

The constants C_{11}, C_{111}, C_{1111}, C_{22}, C_{222}, C_{2222}, and C_{12} are associated with the tensile behavior of flexible composites and are determined by unidirectional tensile tests. Consider a composite lamina under a unidirectional load (i.e. $\Pi_{11} \neq 0$, $\Pi_{22} = 0$ and

Fig. 9.18. Comparisons between theoretical predictions and experimental results of the ratio λ_2/λ_1 of $[\pm\theta_o]_s$ Kevlar/silicone elastomer composite laminates under uniaxial load. (After Luo and Chou 1989.)

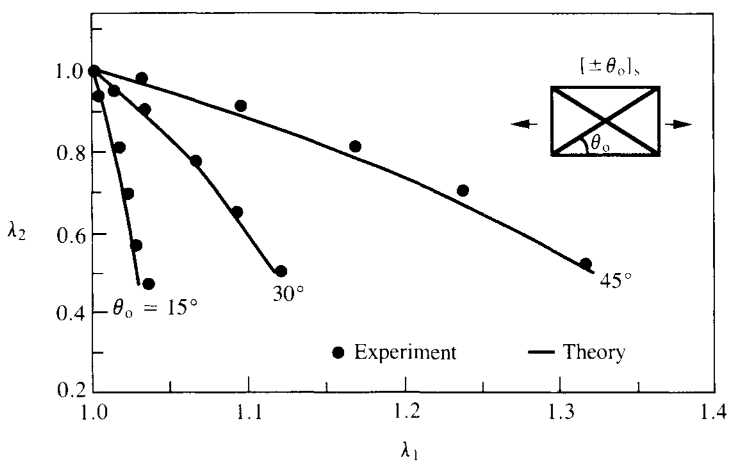

$\Pi_{12}=0$). For $\theta_o=0°$, Eqs. (9.47) and (9.60) yield

$$
\begin{aligned}
\Pi_{11}/\lambda_1 &= C_{11}\left(\frac{\lambda_1^2-1}{2}\right)+C_{111}\left(\frac{\lambda_1^2-1}{2}\right)^2 \\
&\quad + C_{1111}\left(\frac{\lambda_1^2-1}{2}\right)^3+C_{12}\left(\frac{\lambda_2^2-1}{2}\right) \\
\Pi_{22} &= 0 = C_{22}\left(\frac{\lambda_2^2-1}{2}\right)+C_{222}\left(\frac{\lambda_2^2-1}{2}\right)^2 \\
&\quad + C_{2222}\left(\frac{\lambda_2^2-1}{2}\right)^3+C_{12}\left(\frac{\lambda_1^2-1}{2}\right) \\
\Pi_{12} &= \Pi_{21}=0=W_{12}
\end{aligned}
\tag{9.92}
$$

For $\theta_o=90°$, Eqs. (9.47) and (9.60) yield

$$
\begin{aligned}
\Pi_{11}/\lambda_1 &= C_{22}\left(\frac{\lambda_1^2-1}{2}\right)+C_{222}\left(\frac{\lambda_1^2-1}{2}\right)^2 \\
&\quad + C_{2222}\left(\frac{\lambda_1^2-1}{2}\right)^3+C_{12}\left(\frac{\lambda_2^2-1}{2}\right) \\
\Pi_{22} &= 0 = C_{11}\left(\frac{\lambda_2^2-1}{2}\right)+C_{111}\left(\frac{\lambda_2^2-1}{2}\right)^2 \\
&\quad + C_{1111}\left(\frac{\lambda_2^2-1}{2}\right)^3+C_{12}\left(\frac{\lambda_1^2-1}{2}\right) \\
\Pi_{12} &= \Pi_{21}=0=W_{12}
\end{aligned}
\tag{9.93}
$$

Π_{11}, λ_1 and λ_2 are measured experimentally from both $\theta_o=0°$ and 90° unidirectional tensile tests. The constants C_{11}, C_{12}, and C_{22} in Eqs. (9.92) and (9.93) are related to the initial slope of these experimental curves of Π_{11}/λ_1 vs. $(\lambda_1^2-1)/2$. The constants C_{111} and C_{222} are the nonlinear terms associated with the bi-modulus properties of the composite; and the constants C_{1111} and C_{2222} are the fourth-order nonlinear terms in Eq. (9.44). C_{111}, C_{222}, C_{1111}, and C_{22222} are determined by fitting the theoretical curves of Eqs. (9.92) and (9.93) to the longitudinal and transverse experimental curves of Π_{11}/λ_1 vs. $(\lambda_1^2-1)/2$, respectively.

9.3.4.2 *Shear properties*

C_{66} and C_{6666} are the elastic constants associated with the shear properties. Two test methods have been used for characterizing the shear behavior: (1) three-rail 0° simple shear, and (2) simple tension of $[\pm 45°]_s$ specimen.

First, consider the simple shear test in which the applied shear force is parallel to the fiber direction. From Eqs. (9.64), for $\theta = 0$,

$$\begin{aligned}\Pi_{21} &= KW_{22} + \tfrac{1}{2}W_{12} \\ &= K(C_{22}\bar{E}_2 + C_{222}\bar{E}_2^2 + C_{2222}\bar{E}_2^3) + C_{66}\bar{E}_6 + C_{6666}\bar{E}_6^3 \\ &= K^3(C_{22} + \tfrac{1}{2}C_{222}K^2 + \tfrac{1}{8}C_{2222}K^4) + C_{66}K + C_{6666}K^3\end{aligned} \tag{9.94}$$

Since the values of C_{22}, C_{222} and C_{2222} are already known from tensile property measurements, C_{66} and C_{6666} can be determined by fitting the experimental data of Π_{21} vs. K.

Next, consider the tensile test using $[\pm 45°]_s$ specimens. For a $[\pm 45°]_s$ laminate specimen under a tensile load, Eqs. (9.84) can be rewritten as

$$N_{11}/h\lambda_1 = C_{66}(\lambda_1^2 - \lambda_2^2) + \tfrac{1}{4}C_{6666}(\lambda_1^2 - \lambda_2^2)^3 \tag{9.95}$$

By measuring h, N_{11}, λ_1 and λ_2, the curve of $N_{11}/h\lambda_1$ vs. $(\lambda_1^2 - \lambda_2^2)$ can be determined experimentally. Then a curve fitting method can be used to identify the constants C_{66} and C_{6666}. Experiments using both simple shear and tensile tests on Kevlar-49/silicone elastomer composites have yielded comparable results of the elastic constants as shown in Table 9.1.

The tensile experiment on $[\pm 45]_s$ specimens has been quite often used to determine the shear modulus of conventional rigid polymer composites (see ASTM Standard D 3518-76). The basic equation for this experiment is

$$\sigma_{xx}/2 = G_{12}(\varepsilon_{xx} - \varepsilon_{yy}) \tag{9.96}$$

where the engineering stress (σ_{xx}) and strains $(\varepsilon_{xx}$ and $\varepsilon_{yy})$ are measured experimentally.

In order to compare Eq. (9.95) with Eq. (9.96) the following relations are introduced:

$$\begin{aligned}&\lambda_1 = 1 + \varepsilon_{xx} \\ &\lambda_2 = 1 + \varepsilon_{yy} \\ &\frac{N_{11}}{2h\lambda_1} = \frac{\Pi_{xx}}{2}\frac{1}{\lambda_1} = \frac{\sigma_{xx}}{2}\frac{\lambda_2}{\lambda_1}\end{aligned} \tag{9.97}$$

Substitution of Eqs. (9.97) into Eq. (9.95) gives

$$\frac{\sigma_{xx}}{2}=\frac{1+\varepsilon_{xx}}{1+\varepsilon_{yy}}[C_{66}[(\varepsilon_{xx}-\varepsilon_{yy})+(\varepsilon_{xx}^2-\varepsilon_{yy}^2)] \\ +C_{6666}[(\varepsilon_{xx}-\varepsilon_{yy})+(\varepsilon_{xx}^2-\varepsilon_{yy}^2)]^3 \tag{9.98a}$$

For linear elastic materials (i.e. $C_{6666}=0$) under small deformation, and by neglecting the higher order terms of strain, Eq. (9.98a) can be rewritten as

$$\frac{\sigma_{xx}}{2}=\frac{1+\varepsilon_{xx}}{1+\varepsilon_{yy}}[C_{66}(\varepsilon_{xx}-\varepsilon_{yy})] \tag{9.98b}$$

Since the initial shear modulus $G_{12}=C_{66}$, the difference between Eqs. (9.96) and (9.98b) is the geometric factor $(1+\varepsilon_{xx})/(1+\varepsilon_{yy})$. Obviously, for infinitesimal deformation $(1+\varepsilon_{xx})/(1+\varepsilon_{yy})=1$ and Eqs. (9.96) and (9.98b) are identical. However, if the deformation is not infinitesimal, G_{12} determined from Eq. (9.96) may not be accurate because of the omission of the geometric factor. For instance, let the strain $\varepsilon_{xx}=0.02$ and use the relation of Eq. (9.98a); the error is $(1+\varepsilon_{xx})/(1+\varepsilon_{yy})=4.1\%$.

The elastic constants of Kevlar-49/silicone elastomer obtained from the above methods are listed in Table 9.1. The higher order elastic constants (i.e. C_{iii} and C_{iiii}) are determined by a regression curve fitting to the experimental data. Thus, they are valid only within the strain level at which they are obtained experimentally.

9.4 Constitutive relations based on the Eulerian description

In the above, the Lagrangian system has been used to derive the closed form constitutive equations for flexible composites, based upon a strain-energy function, for both lamina and laminate. These equations can be used to predict the nonlinear elastic behavior of flexible composites under different cases of finite deformation. It should be mentioned that the Lagrangian stress, defined as force per undeformed area, is a nominal stress and the real force equilibrium is established in the deformed or contemporary configuration. Furthermore, the anisotropic elastic properties of the composite always refer to the deformed configuration. For example, the current Young's modulus describes the stiffness in the current fiber direction which rotates during deformation. Therefore, in some cases, it is convenient to use the deformed body as the reference to describe the constitutive relation.

In this section, a nonlinear constitutive relation has also been developed based upon the Eulerian description where the deformed configuration of the composite is used as the reference state (Luo and Chou 1988a). A stress-energy function, referring to the current principal material coordinate $\underset{\sim}{x}$ (Fig. 9.2b), provides the basis for deriving the constitutive relations.

9.4.1 *Stress-energy function*

In finite elasticity, the energy densities in terms of either the Eulerian or Lagrangian stresses are not unique referring to a fixed coordinate; this can be demonstrated through the consideration of a 'rigid-body rotation' (Fung 1969). As an example, consider a bar which is subjected to a simple tension and rotating about the z axis. At one instant, the bar is parallel to the x axis so that $\sigma_{xx} \neq 0$ and $\sigma_{yy} = 0$. At another instant, when the bar becomes parallel to the y axis, the stress state is given by $\sigma_{xx} = 0$ and $\sigma_{yy} \neq 0$. Thus a rigid-body rotation changes the stress tensor, even though the state of stress in the bar remains unchanged. A complementary energy function referring to a fixed coordinate may be defined based upon the second Piola–Kirchhoff stress tensor P_{AB}. However, as indicated in Eq. (9.36), the second Piola–Kirchhoff stress still involves the displacement gradient. Thus, the use of complementary energy in terms of P_{ij} does not really make the constitutive relation simpler.

In order to establish the stress-energy function, a moving Eulerian coordinate system is introduced in this section. Figure 9.2(b) illustrates a unidirectional flexible composite lamina under a finite deformation in the Eulerian system. Unlike Fig. 9.2(a), here the deformed configuration has been chosen as the reference state, and the rectangular element $A'E'F'D'$ in the deformed body is considered. The sides $A'D'$ and $A'E'$ coincide with the current principal material coordinate system l'–t' or $\underset{\sim}{x}_1$–$\underset{\sim}{x}_2$, with l' referring to the current fiber direction. The underline of a quantity refers to the current principal material coordinates $\underset{\sim}{x}_1$–$\underset{\sim}{x}_2$. Thus, the element $AEFD$ corresponds to the element $A'E'F'D'$ in the undeformed state. One may assume that the rectangle $A'E'F'D'$ undergoes two stages of deformation in restoring to its initial shape $AEFD$. These stages are illustrated in Fig. 9.19. First, $A'E'F'D'$ becomes a smaller rectangle $A''E''F''D''$ by removing the normal stresses; then it reverses to $AEFD$ by removing the shear stress.

The deformations depicted in Fig. 9.19 can be related to the Eulerian strain components. Let the line elements $AD = \mathrm{d}l_o$ and $AE = \mathrm{d}t_o$ in the undeformed lamina (Fig. 9.19c); also define

$A'D' = \mathrm{d}l$ and $A'E' = \mathrm{d}t$ in the deformed lamina (Fig. 9.19a). Then, the physical significance of the Eulerian strains can be explained as

$$\begin{aligned} 2\underset{\sim}{e}_{11} &= [(\mathrm{d}l)^2 - (\mathrm{d}l_o)^2]/(\mathrm{d}l)^2 \\ 2\underset{\sim}{e}_{22} &= [(\mathrm{d}t)^2 - (\mathrm{d}t_o)^2]/(\mathrm{d}t)^2 \\ 2\underset{\sim}{e}_{12} &= \sin \underset{\sim}{\gamma}_{12}(\sqrt{(1 - 2\underset{\sim}{e}_{11})}\sqrt{(1 - 2\underset{\sim}{e}_{22})}) \end{aligned} \tag{9.99}$$

where $\underset{\sim}{e}_{ij}$ are the Eulerian strains referring to the current principal material coordinates $\underset{\sim}{x}_1$–$\underset{\sim}{x}_2$, and $\underset{\sim}{\gamma}_{12}$ is the angular deviation from a right-angle as shown in Fig. 9.19.

The stress-energy per unit area of the deformed lamina ($A'E'F'D'$) is assumed to be a function of the Eulerian stress components referring to the current principal material coordinate

Fig. 9.19. Illustration of the deformation of a rectangular element in the Eulerian system. (After Luo and Chou 1988a.)

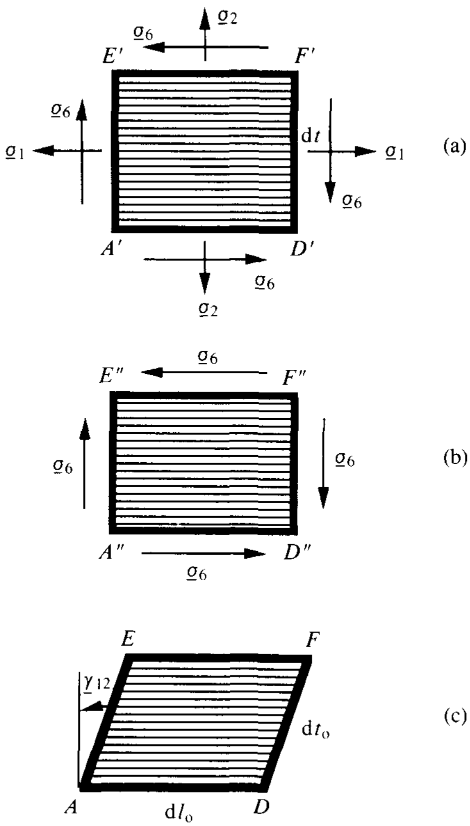

$\underset{\sim}{x}_1$–$\underset{\sim}{x}_2$, namely $W^* = W^*(\underset{\sim}{\sigma}_{11}, \underset{\sim}{\sigma}_{22}, \underset{\sim}{\sigma}_{12}^2)$. The following expression is adopted:

$$\begin{aligned} W^* = {} & \tfrac{1}{2}S_{11}\underset{\sim}{\sigma}_1^2 + \tfrac{1}{3}S_{111}\underset{\sim}{\sigma}_1^3 + \tfrac{1}{4}S_{1111}\underset{\sim}{\sigma}_1^4 \\ & + S_{12}\underset{\sim}{\sigma}_1\underset{\sim}{\sigma}_2 + \tfrac{1}{2}S_{22}\underset{\sim}{\sigma}_2^2 + \tfrac{1}{3}S_{222}\underset{\sim}{\sigma}_2^3 \\ & + \tfrac{1}{4}S_{2222}\underset{\sim}{\sigma}_2^4 + \tfrac{1}{2}S_{66}\underset{\sim}{\sigma}_6^2 + \tfrac{1}{4}S_{6666}\underset{\sim}{\sigma}_6^4 \\ & + S_{166}\underset{\sim}{\sigma}_1\underset{\sim}{\sigma}_6^2 + S_{2266}\underset{\sim}{\sigma}_2^2\underset{\sim}{\sigma}_6^2 \end{aligned} \tag{9.100}$$

where $\underset{\sim}{\sigma}_i$ are the Eulerian stresses referring to the current principal material coordinates $\underset{\sim}{x}_1$–$\underset{\sim}{x}_2$. Also, the short-handed notations are used, i.e. $\underset{\sim}{\sigma}_1 = \underset{\sim}{\sigma}_{11}$, $\underset{\sim}{\sigma}_2 = \underset{\sim}{\sigma}_{22}$ and $\underset{\sim}{\sigma}_6 = \underset{\sim}{\sigma}_{12}$. S_{ij}, S_{ijk} and S_{ijkl} are the compliance constants. Equation (9.100) is similar to the expressions of Hahn and Tsai (1973) in their mathematical forms. However, due to the finite deformation, it should be mentioned that: (1) The Eulerian coordinate $\underset{\sim}{x}$ used here is a moving coordinate, which is chosen to coincide with the current fiber longitudinal and transverse directions, l' and t'. Therefore, the energy function satisfies the test of rigid-body rotation. (2) The Eulerian stresses, $\underset{\sim}{\sigma}_{ij}$, used in the energy function are the current stress state of the deformed lamina.

9.4.2 *General constitutive equations*

The complementary energy per unit volume of a deformed a lamina is $W^* = \underset{\sim}{\sigma}_{ij}\underset{\sim}{e}_{ij} - W(\underset{\sim}{e}_{ij})$. Here, $W(\underset{\sim}{e}_{ij}) = \underset{\sim}{\sigma}_{ij}\delta\underset{\sim}{e}_{ij}$ is the strain-energy density. Then,

$$\delta W^* = \underset{\sim}{\sigma}_{ij}\delta\underset{\sim}{e}_{ij} + \underset{\sim}{e}_{ij}\delta\underset{\sim}{\sigma}_{ij} - \frac{\partial W}{\partial \underset{\sim}{e}_{ij}}\delta\underset{\sim}{e}_{ij} \tag{9.101}$$

Since

$$\underset{\sim}{\sigma}_{ij} = \frac{\partial W}{\partial \underset{\sim}{e}_{ij}}, \tag{9.102}$$

the following can be obtained from Eq. (9.101):

$$\delta W^* = \underset{\sim}{e}_{ij}\delta\underset{\sim}{\sigma}_{ij} \tag{9.103}$$

or

$$\underset{\sim}{e}_{ij} = \frac{\partial W^*}{\partial \underset{\sim}{\sigma}_{ij}} \tag{9.104}$$

Substituting Eq. (9.100) into Eq. (9.104), the Eulerian strain components referring to the coordinates $\underset{\sim}{x}_1$–$\underset{\sim}{x}_2$ are obtained as

$$
\begin{aligned}
\underset{\sim}{e}_1 &= S_{11}\underset{\sim}{\sigma}_1 + S_{111}\underset{\sim}{\sigma}_1^2 + S_{1111}\underset{\sim}{\sigma}_1^3 + S_{12}\underset{\sim}{\sigma}_2 + S_{166}\underset{\sim}{\sigma}_6^2 \\
\underset{\sim}{e}_2 &= S_{22}\underset{\sim}{\sigma}_2 + S_{222}\underset{\sim}{\sigma}_2^2 + S_{2222}\underset{\sim}{\sigma}_2^3 + S_{12}\underset{\sim}{\sigma}_1 + 2S_{2266}\underset{\sim}{\sigma}_2\underset{\sim}{\sigma}_6^2 \\
\underset{\sim}{e}_6 &= S_{66}\underset{\sim}{\sigma}_6 + S_{6666}\underset{\sim}{\sigma}_6^3 + 2S_{166}\underset{\sim}{\sigma}_1\underset{\sim}{\sigma}_6 + 2S_{2266}\underset{\sim}{\sigma}_2^2\underset{\sim}{\sigma}_6
\end{aligned}
\tag{9.105}
$$

Here $\underset{\sim}{e}_1 = \underset{\sim}{e}_{11}$, $\underset{\sim}{e}_2 = \underset{\sim}{e}_{22}$, $\underset{\sim}{e}_6 = 2\underset{\sim}{e}_{12}$. The choice of compliance constants in Eq. (9.100) is made on the following basis. First, S_{11}, S_{22}, S_{12} and S_{66} are associated with the linear deformation. Second, the terms S_{11} and S_{222} are adopted for representing the bi-modulus behavior in the axial and transverse directions, respectively. Third, the nonlinear deformations are represented by S_{1111}, S_{2222} and S_{6666}. Lastly, the greatest uncertainty involves the coupling terms between the normal and shear deformations. Unlike in rigid composites, the coupling effects may not be negligible in flexible composites. Two terms, S_{166} and S_{2266}, are retained to represent the interactions between axial and shear deformations in Eqs. (9.105).

Having established the constitutive relations with respect to the principal material coordinates $\underset{\sim}{x}_1$–$\underset{\sim}{x}_2$, the general constitutive relations of a composite lamina referring to the fixed coordinates x_1–x_2 (Fig. 9.2b) can be derived from Eq. (9.105) and the tensor transformation relation,

$$
[e] = [T]^{\mathrm{T}}[\mathbf{S}][T][\sigma] = [\mathbf{S}^*][\sigma] \tag{9.106}
$$

where

$$
[\mathbf{S}] = \begin{bmatrix} S_{11} + S_{111}\underset{\sim}{\sigma}_1 + S_{1111}\underset{\sim}{\sigma}_1^2 & S_{12} & S_{166}\underset{\sim}{\sigma}_6 \\ S_{12} & S_{22} + S_{222}\underset{\sim}{\sigma}_2 + S_{2222}\underset{\sim}{\sigma}_2^2 & 2S_{2266}\underset{\sim}{\sigma}_2\underset{\sim}{\sigma}_6 \\ 2S_{166}\underset{\sim}{\sigma}_6 & 2S_{2266}\underset{\sim}{\sigma}_2\underset{\sim}{\sigma}_6 & S_{66} + S_{6666}\underset{\sim}{\sigma}_6^2 \end{bmatrix}
$$

$$
\{e\} = \begin{Bmatrix} e_1 \\ e_2 \\ e_6 \end{Bmatrix}, \qquad \{\sigma\} = \begin{Bmatrix} \sigma_1 \\ \sigma_2 \\ \sigma_6 \end{Bmatrix}, \quad \text{and} \quad [T] = \begin{bmatrix} c^2 & s^2 & 2cs \\ s^2 & c^2 & -2cs \\ -cs & cs & c^2 - s^2 \end{bmatrix}
$$

Here, $c = \cos\theta$ and $s = \sin\theta$, where θ denotes the current fiber orientation angle. Also, e_i and σ_i are, respectively, the Eulerian stress and strain referring to the coordinates x_1–x_2. The full expression of $[\mathbf{S}^*]$ in Eq. (9.106) is

$$
\begin{aligned}
[\mathbf{S}^*] &= \begin{bmatrix} \mathbf{S}^*_{11} & \mathbf{S}^*_{12} & \mathbf{S}^*_{16} \\ \mathbf{S}^*_{21} & \mathbf{S}^*_{22} & \mathbf{S}^*_{26} \\ \mathbf{S}^*_{61} & \mathbf{S}^*_{62} & \mathbf{S}^*_{66} \end{bmatrix} \\
&= \begin{bmatrix}
\begin{matrix} c^4S_{11} + 2c^2s^2S_{12} \\ +s^4S_{22} + c^2s^2S_{66} \end{matrix} & \begin{matrix} c^2s^2S_{11} + (c^4+s^4)S_{12} \\ +c^2s^2S_{22} - c^2s^2S_{66} \end{matrix} & \begin{matrix} 2c^3sS_{11} - 2cs(c^2-s^2)S_{12} \\ -2cs^3S_{22} - cs(c^2-s^2)S_{66} \end{matrix} \\
\begin{matrix} c^2s^2S_{11} + (c^4+s^4)S_{12} \\ +c^2s^2S_{22} - c^2s^2S_{66} \end{matrix} & \begin{matrix} s^4S_{11} + 2c^2s^2S_{12} \\ +c^4S_{22} + c^2s^2S_{66} \end{matrix} & \begin{matrix} 2cs^3S_{11} + 2cs(c^2-s^2)S_{12} \\ -2c^3sS_{22} + cs(c^2-s^2)S_{66} \end{matrix} \\
\begin{matrix} c^3sS_{11} - cs(c^2-s^2)S_{12} \\ -cs^3S_{22} - \frac{1}{2}cs(c^2-s^2)S_{66} \end{matrix} & \begin{matrix} cs^3S_{11} + cs(c^2-s^2)S_{12} \\ -c^3sS_{22} + \frac{1}{2}cs(c^2-s^2)S_{66} \end{matrix} & \begin{matrix} 2c^2s^2S_{11} - 4c^2s^2S_{12} \\ +2c^2s^2S_{22} + \frac{1}{2}(c^2-s^2)S_{66} \end{matrix}
\end{bmatrix} \\
&\quad + (S_{111}\sigma_1 + S_{111}\sigma_1^2)\begin{bmatrix} c^4 & c^2s^2 & 2c^3s \\ c^2s^2 & c^2s^2 & 2cs^3 \\ c^3s & cs^3 & 2c^2s^2 \end{bmatrix} \\
&\quad + (S_{222}\sigma_2 + S_{222}\sigma_2^2)\begin{bmatrix} s^4 & c^2s^2 & -2cs^3 \\ c^2s^2 & c^2s^2 & -2c^3s \\ -cs^3 & -c^3s & 2c^2s^2 \end{bmatrix} \\
&\quad + s_{6666}\sigma_6^2\begin{bmatrix} c^2s^2 & -c^2s^2 & -cs(c^2-s^2) \\ -c^2s^2 & -c^2s^2 & cs(c^2-s^2) \\ -\frac{1}{2}cs(c^2-s^2) & \frac{1}{2}cs(c^2-s^2) & \frac{1}{2}(c^2-s^2) \end{bmatrix} \\
&\quad + S_{166}\sigma_6\begin{bmatrix} -3c^3s & c^3s - 2cs^3 & c^4 - 5c^2s^2 \\ 2c^3s - 2cs^3 & 3cs^3 & -s^4 + 5c^2s^2 \\ c^4 - 2c^2s^2 & -s^4 + 2c^2s^2 & 3c^3s - 3cs^3 \end{bmatrix} \\
&\quad + S_{2266}\sigma_2\sigma_6\begin{bmatrix} -4cs^3 & 2cs^3 - 2c^3s & -2s^4 + 6c^2s^2 \\ 2cs^3 - 2c^3s & 4c^3s & 2c^4 - 6c^2s^2 \\ -s^4 + 3c^2s^2 & c^4 - 3c^2s^2 & 4cs^3 - 4c^3s \end{bmatrix}
\end{aligned} \tag{9.107}
$$

The stresses in the current principal material directions, $\underset{\sim}{\sigma}_i$, are also obtained as

$$[\underset{\sim}{\sigma}] = [T][\sigma] \tag{9.108}$$

Referring to Fig. 9.2(b) the current fiber orientation angle is

$$\theta = \theta_o + \Delta\theta \tag{9.109}$$

The fiber reorientation angle ($\Delta\theta$) due to finite deformation can be determined as follows. First, the angles DAD' and EAE' are defined as α and β, respectively. Then,

$$\Delta\theta = (\alpha+\beta)/2 + (\alpha-\beta)/2 \tag{9.110}$$

Here, the symmetric part of $\Delta\theta$, $(\alpha+\beta)/2$, equals $\underline{\gamma}_{12}/2$; the antisymmetric part of $\Delta\theta$, $(\alpha-\beta)/2$, is defined as ω. It is understood that ω is the rigid-body rotation, which is independent of the coordinate system but dependent on the boundary conditions. If ω can be expressed in terms of the strain tensors, from Eqs. (9.99) and (9.110)

$$\Delta\theta = \frac{1}{2}\sin^{-1}\left(\frac{2\underline{e}_{12}}{\sqrt{(1-2\underline{e}_{11})}\sqrt{(1-2\underline{e}_{22})}}\right) + \omega(\underline{e}_{ij}) \tag{9.111}$$

Introducing Eq. (9.111) into Eq. (9.109), the current fiber orientation angle θ is expressed as a function in terms of the strain tensor. Then the general constitutive relations can be completely determined from Eqs. (9.106) and (9.111). The following are two illustrative examples.

9.4.3 *Pure homogeneous deformation*

The pure homogeneous deformation, with principal extension ratios λ_1 and λ_2 defined along the axes of the fixed coordinate system X, is shown in Fig. 9.7 and described by Eqs. (9.56). Referring to Eqs. (9.14) and (9.20),

$$[g] = \begin{bmatrix} \lambda_1 & 0 \\ 0 & \lambda_2 \end{bmatrix}, \qquad [g]^{-1} = \begin{bmatrix} \dfrac{1}{\lambda_1} & 0 \\ 0 & \dfrac{1}{\lambda_2} \end{bmatrix} \tag{9.112}$$

and

$$2[e] = \begin{bmatrix} 1-\left(\dfrac{1}{\lambda_1}\right)^2 & 0 \\ 0 & 1-\left(\dfrac{1}{\lambda_2}\right)^2 \end{bmatrix} \tag{9.113}$$

Eq. (9.113) gives

$$\lambda_1 = \frac{1}{\sqrt{(1-2e_{11})}}$$
$$\lambda_2 = \frac{1}{\sqrt{(1-2e_{22})}} \tag{9.114}$$

Referring to Fig. 9.7 the current fiber orientation can also be written as

$$\theta = \tan^{-1}\left\{\frac{\lambda_2 \sin\theta_o}{\lambda_1 \cos\theta_o}\right\} = \tan^{-1}\left\{\frac{\lambda_2}{\lambda_1}\tan\theta_o\right\} \tag{9.115}$$

Substituting Eqs. (9.114) into Eq. (9.115),

$$\theta = \tan^{-1}\left\{\frac{\sqrt{(1-2e_{11})}}{\sqrt{(1-2e_{22})}}\tan\theta_o\right\} \tag{9.116}$$

The substitution of Eq. (9.116) into Eq. (9.106) results in three independent equations. It is known from Eq. (9.113) that $e_{12}=0$. Thus, by giving any two values of the following five variables in Eq. (9.106): stresses σ_1, σ_2, σ_6, and strains e_1, e_2 (or λ_1 and λ_2), the remaining three can be solved.

Finally, it is worth noting that from Eqs. (9.35) and (9.112), the Lagrangian stresses can be written in terms of the Eulerian stresses as

$$\begin{aligned} \Pi_{11} &= \lambda_2\sigma_{11} \\ \Pi_{22} &= \lambda_1\sigma_{22} \\ \Pi_{12} &= \lambda_2\sigma_{12} \\ \Pi_{21} &= \lambda_1\sigma_{12} \end{aligned} \tag{9.117}$$

9.4.4 *Simple shear superposed on simple extension*

The deformation of 'simple shear superposed on simple extension' (Case 1) is shown in Fig. 9.12(a) and expressed by Eqs. (9.67). Using Eqs. (9.14) and (9.20), it can be found

$$[\mathbf{g}] = \begin{bmatrix} \lambda_1 & K\lambda_2 \\ 0 & \lambda_2 \end{bmatrix}, \qquad [\mathbf{g}]^{-1} = \begin{bmatrix} \dfrac{1}{\lambda_1} & -\dfrac{K}{\lambda_1} \\ 0 & \dfrac{1}{\lambda_2} \end{bmatrix} \tag{9.118}$$

and

$$2[\mathbf{e}] = \begin{bmatrix} 1 - \left(\dfrac{1}{\lambda_1}\right)^2 & \dfrac{K}{\lambda_1^2} \\ \dfrac{K}{\lambda_1^2} & 1 - \left[\left(\dfrac{K}{\lambda_1}\right)^2 + \left(\dfrac{1}{\lambda_2}\right)^2\right] \end{bmatrix} \tag{9.119}$$

Invert the above equation to obtain

$$\begin{aligned} \lambda_1 &= \frac{1}{\sqrt{(1-2e_{11})}} \\ \lambda_2 &= \frac{\sqrt{(1-2e_{11})}}{\sqrt{[(1-2e_{11})(1-2e_{22})-4e_{12}^2]}} \\ K &= \frac{2e_{12}}{1-2e_{11}} \end{aligned} \tag{9.120}$$

Also, referring to Fig. 9.12(a), the current fiber orientation can be expressed as

$$\theta = \tan^{-1}\left(\frac{x_2}{x_1}\right) = \tan^{-1}\left(\frac{\lambda_2 \tan\theta_o}{\lambda_1 + \lambda_2 K \tan\theta_o}\right) \tag{9.121}$$

The substitution of Eq. (9.121) into Eq. (9.106), results in three independent equations. If the values are known for any three of the following six variables: stresses σ_1, σ_2, σ_6, and strains e_1, e_2, e_6 (or λ_1, λ_2 and K), the remaining three can be solved.

As mentioned in Section 9.3.2.5, for an off-axis specimen under uniaxial loading, with a length/width ratio $\gg 1$, the central lines of the middle section of the specimen remain straight in the loading direction. Then, this deformation can be referred to as 'simple shear superposed on simple extension (Case 1)'. Using the uniaxial loading conditions, $\sigma_{11} \neq 0$, $\sigma_{22} = \sigma_{21} = 0$, and Eqs. (9.106), (9.120) and (9.121), the deformation parameters λ_1, λ_2, and K (or e_{ij}) can be solved.

Figure 9.20 shows the comparison between analytical predictions and experimental results for the off-axis responses of Kevlar/elastomer composites under simple tension based upon the Eulerian approach. The fiber initial orientations are 10°, 30° and 60°. The same comparisons for tirecord/rubber composite specimens are shown in Fig. 9.21. The fiber initial orientations are 15°, 30° and 60° in this case. The predicted results are based upon Eqs. (9.106), (9.120) and (9.121) and an iterative calculation method. The elastic constants are shown in Table 9.1.

9.4.5 *Determination of elastic compliance constants*

The compliance constants in Eq. (9.100) can be determined experimentally (Luo and Chou 1988a). The second-order constants (S_{11}, S_{22}, S_{12} and S_{66}) are based on the linear behavior. The other constants are obtained by fitting the theoretical curves to experimental data. For example, for unidirectional tensile test in the $\underline{x}_1$ direction (i.e. $\underline{\sigma}_1 \neq 0$ and $\underline{\sigma}_2 = \underline{\sigma}_6 = 0$), Eq. (9.105) becomes

$$\underline{e}_1 = S_{11}\underline{\sigma}_1 + S_{111}\underline{\sigma}_1^2 + S_{1111}\underline{\sigma}_1^3 \tag{9.122}$$

where the underline denotes the current principal material coordinate. Then, S_{11} is obtained from the initial slope of the experimental $\underline{\sigma}_1$–$\underline{e}_1$ curve (i.e. $S_{11} = 1/$Young's modulus). S_{111} (which reflects bi-modulus behavior) and S_{1111} are determined by fitting the theoretical curves to experimental data in both tension and compression. With the unidirectional load applied in the $\underline{x}_2$ direction, S_{22}, S_{222} and S_{2222}, can be determined by the same procedures as in the $\underline{x}_1$ direction.

Fig. 9.20. Comparisons between theoretical predictions and experimental results of 10°, 30° and 60° off-axis stress–strain response of Kevlar/silicone elastomer composite laminae (Eulerian description). (After Luo and Chou 1988a.)

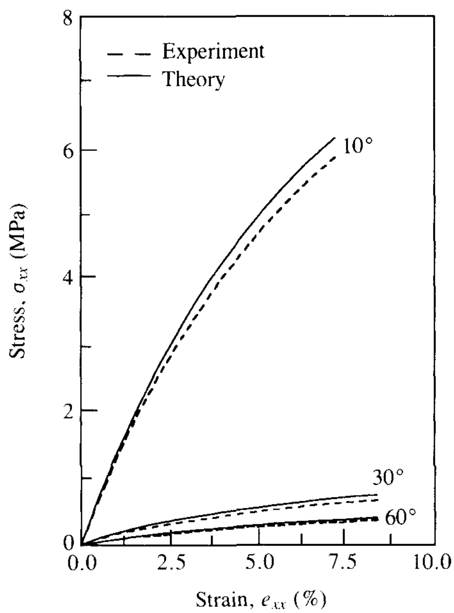

The remaining constants are related to shear (S_{66} and S_{6666}) and stretching–shear coupling (S_{166} and S_{2266}). If S_{166} and S_{2266} are negligibly small, the shear constants can be determined experimentally as described in Section 9.3.4.2, with proper stress and strain transformations from the Lagrangian system into the Eulerian system as described in Section 9.2.2.

The shear constants including the stretching–shear coupling listed in Table 9.1 are obtained by off-axis tensile tests at various fiber off-axis angles. For the unidirectional tensile condition ($\sigma_{11} \neq 0$, $\sigma_{22} = \sigma_{12} = 0$), Eq. (9.106) can be rewritten as

$$[c^4 S_{11} + 2c^2 s^2 S_{12} + s^4 S_{22}]\sigma_{11}/(cs) - e_{11}/(cs)$$
$$= S_{66}\underset{\sim}{\sigma}_6 + S_{6666}\underset{\sim}{\sigma}_6^3 - (3c/s)S_{166}\underset{\sim}{\sigma}_6^2 + (4s/c)S_{2266}\underset{\sim}{\sigma}_6^3 \quad (9.123)$$

where $c = \cos\theta$ and $s = \sin\theta$, $\underset{\sim}{\sigma}_6 = cs\sigma_{11}$. The fiber orientation angle, θ, and the stress–strain relations are measured experimentally. In Eq. (9.123), there are four unknown constants, S_{66}, S_{6666}, S_{166} and S_{2266}. The relations between $\underset{\sim}{\sigma}_6$ and the values of Eq. (9.123) which are determined by experimental measurements of σ_{11},

Fig. 9.21. Comparisons between theoretical predictions and experimental results of 15°, 30° and 60° off-axis stress–strain response of tirecord/rubber composite laminae (Eulerian description). (After Luo and Chou 1988a.)

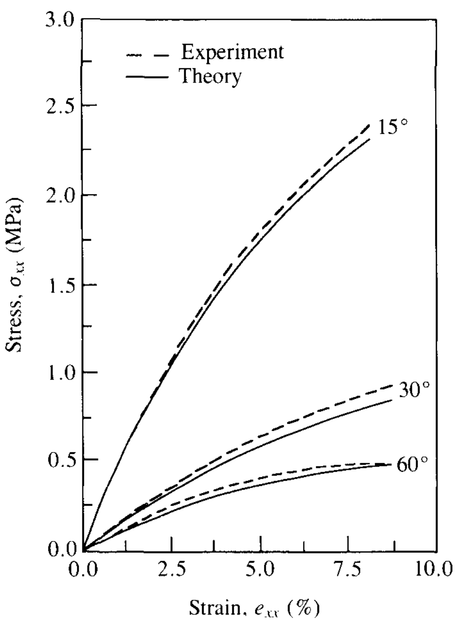

e_{11}, θ and the elastic constants related to the tensile properties (S_{11}, S_{12} and S_{22}). S_{66} is the initial slope of the stress–strain curve. Given sufficient experimental data (the number of specimens with different initial fiber orientations should be larger than the number of unknown constants), the remaining compliance constants S_{6666}, S_{166} and S_{2266} can be determined by a regression technique to fit the theoretical curve of Eq. (9.123) to the experimental curves.

9.5 Elastic behavior of flexible composites reinforced with wavy fibers

9.5.1 *Introduction*

In Chapter 8, an iso-phase model for flexible composites containing sinusoidally shaped fibers (Fig. 8.13) is presented and the analysis of the elastic behavior of such composites is based upon a step-wise incremental technique and the classical lamination theory. Being a well established analytical technique, the lamination theory does provide a convenient tool for describing the basic characteristics of flexible composites. However, because of the use of superposition techniques for nonlinear finite deformation problems, the limitation of incremental analysis is obvious. In an effort to provide a rigorous treatment, Luo and Chou (1988a&b, 1990b) applied the constitutive models based upon the Lagrangian (Section 9.3) and Eulerian descriptions (Section 9.4) to study the nonlinear elastic behavior of flexible composites with wavy fibers under finite deformation.

The deformation of the iso-phase flexible composite (see Fig. 8.13) is best understood by examining a representative element which contains a full wavelength of the sinusoidal curve (Fig. 9.22). This element is further divided into sub-elements along the x_1 axis. Each sub-element of the composite between x_1 and $x_1 + \Delta x_1$ is approximated by an off-axis unidirectional fiber composite, in which fibers are inclined at an angle $\theta_o^{(n)}$ to the x_1 axis. Referring to Eq. (8.14), the initial fiber orientation of sub-element (n), for example, is given as

$$\theta_o^{(n)} = \frac{1}{2}\left[\tan^{-1}\left(\frac{2\pi a}{\lambda}\cos\frac{2\pi x_1}{\lambda}\right) + \tan^{-1}\left(\frac{2\pi a}{\lambda}\cos\frac{2\pi(x_1+\Delta x_1)}{\lambda}\right)\right] \tag{9.124}$$

It is also assumed that the stress and strain of a sub-element are homogeneous under axial loading. This assumption is supported by the photoelastic analysis (Luo and Chou 1988a). Figure 9.23 is a photoelastic view of a flexible composite sample under longitudinal loading; it shows that relatively uniform strain is maintained in distinct regions along the longitudinal direction. It should be noted that although all the experimental data collected are based upon a Kevlar-49/silicone elastomer system, the photograph shown in Fig. 9.23 is based upon graphite fiber as a reinforcement materials, so better contrast between the fiber and matrix in the photograph can be achieved.

Based upon the above assumptions, the analysis for the iso-phase model consists of two steps: (1) The constitutive relation of an off-axis sub-element under finite deformation is examined based upon the analysis developed in Sections 9.3 and 9.4. (2) The total deformation of the composite is the summation of the deformations of all these sub-elements.

9.5.2 *Longitudinal elastic behavior based on the Lagrangian approach*

Under the uniaxial tensile force F_1 in the x_1 direction, the following plane stress condition of the flexible composite is

Fig. 9.22. Deformation of a sub-element of a flexible composite containing sinusoidally shaped fibers under longitudinal tension. (After Luo and Chou 1990b.)

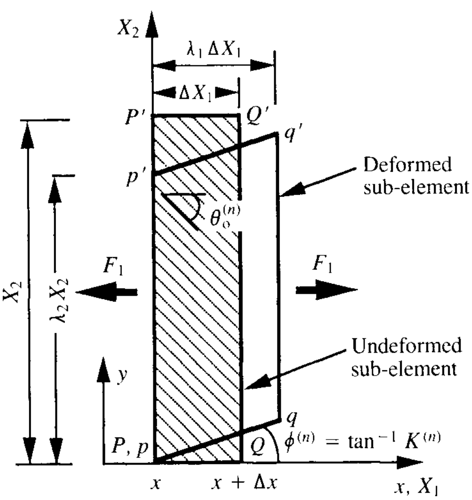

assumed:

$$\Pi_{11} = F_1/A_o$$
$$\Pi_{22} = 0 \tag{9.125}$$
$$\Pi_{21} = 0$$

where A_o is the initial cross-sectional area perpendicular to the x_1 axis.

Figure 9.22 shows the deformation of a typical sub-element $PQQ'P'$. $pqq'p'$ represents the configuration in the deformed state. Due to the iso-phase fiber arrangement, the edge qq' remains perpendicular to the X_1 axis. Let $x_i^{(n)}$ be the coordinates of an arbitrary particle in $PQQ'P'$, and $x_i^{(n)}$ be the corresponding local coordinates of this particle in $pqq'p'$. Here, the superscript refers to the sub-element (n). This deformation is specified as

$$\begin{aligned} x_1^{(n)} &= \lambda_1^{(n)} X_1^{(n)} \\ x_2^{(n)} &= k^{(n)} \lambda_1^{(n)} X_1^{(n)} + \lambda_2^{(n)} X_2^{(n)} \end{aligned} \tag{9.126}$$

Equations (9.126) specify a deformation equivalent to Case 2 of Section 9.3.2.5, namely 'simple shear superposed on simple extension'. Using Eqs. (9.74) and the stress boundary condition of Eqs.

Fig. 9.23. A photoelastic view of a flexible composite lamina under longitudinal tension. (After Luo and Chou 1988a.)

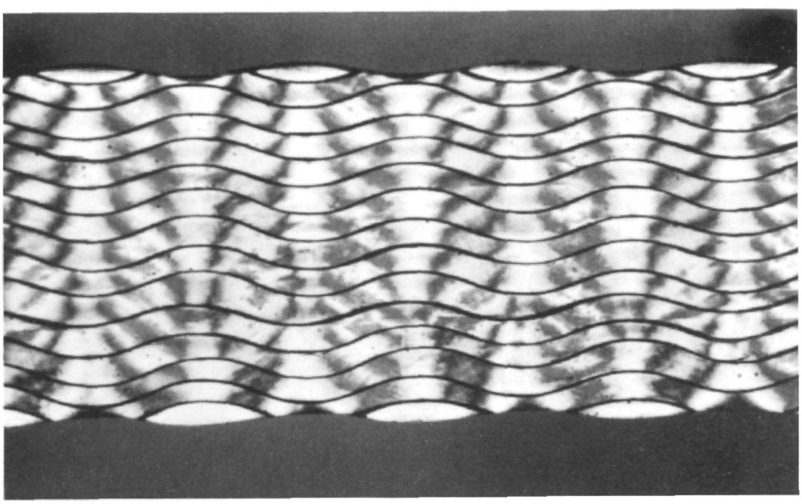

(9.125), the following can be obtained:

$$\begin{aligned} \Pi_{11} &= \lambda_1^{(n)}[c^2 W_{11} + s^2 W_{22} - cs W_{12}] \\ 0 = \Pi_{22} &= s^2 W_{11} + c^2 W_{22} + cs W_{12} \\ 0 = \Pi_{21} &= cs W_{11} - cs W_{22} + \tfrac{1}{2}(c^2 - s^2) W_{12} \end{aligned} \tag{9.127}$$

Here, W_{ij} is a function of $K^{(n)}$, $\lambda_1^{(n)}$ and $\lambda_2^{(n)}$, and it is given by Eqs. (9.47) and (9.73). The initial fiber orientation $\theta_o^{(n)}$ is given by Eq. (9.124). Then, the three unknowns, $K^{(n)}$, $\lambda_1^{(n)}$ and $\lambda_2^{(n)}$ can be solved from Eqs. (9.127). It is interesting to note that Π_{12} does not vanish, and it can be found from Eqs. (9.74)

$$\Pi_{12} = K^{(n)} \Pi_{11} \tag{9.128}$$

The current fiber orientation, $\theta^{(n)}$, of the sub-element (n) (Fig. 9.22) is

$$\theta^{(n)} = \tan^{-1}\left[K^{(n)} + \frac{\lambda_2^{(n)}}{\lambda_1^{(n)}} \tan \theta_o^{(n)} \right] \tag{9.129}$$

The average extension ratio of the wavelength in the X_1 direction can be derived as

$$\lambda_1 = \frac{\Delta x}{\lambda} \sum_{n=1}^{m} \lambda_1^{(n)} \tag{9.130}$$

9.5.3 *Longitudinal elastic behavior based on the Eulerian approach*

Under the uniaxial tension force F_1 in the longitudinal direction, the following stress states in the Eulerian system are assumed:

$$\sigma_{11} = F_1/A, \qquad \sigma_{22} = \sigma_{12} = 0 \tag{9.131}$$

where A is the area of the section perpendicular to the longitudinal direction in the deformed state. From Eqs. (9.126) the deformation of the sub-element (n) can be written in the Eulerian system as

$$\begin{aligned} X_1 &= \frac{1}{\lambda_1^{(n)}} x_1 \\ X_2 &= -\frac{K^{(n)}}{\lambda_2^{(n)}} x_1 + \frac{1}{\lambda_2^{(n)} x_2} \end{aligned} \tag{9.132}$$

Using Eqs. (9.18) and (9.20), it can be found

$$[\mathbf{g}]^{-1} = \begin{bmatrix} \dfrac{1}{\lambda_1^{(n)}} & 0 \\ -\dfrac{K^{(n)}}{\lambda_2^{(n)}} & \dfrac{1}{\lambda_2^{(n)}} \end{bmatrix} \tag{9.133}$$

and

$$2[\mathbf{e}] = \begin{bmatrix} 1 - \left[\left(\dfrac{1}{\lambda_1^{(n)}}\right)^2 - \left(\dfrac{K^{(n)}}{\lambda_2^{(n)}}\right)^2\right] & \dfrac{K^{(n)}}{(\lambda_2^{(n)})^2} \\ \dfrac{K^{(n)}}{(\lambda_2^{(n)})^2} & 1 - \left(\dfrac{1}{\lambda_2^{(n)}}\right)^2 \end{bmatrix} \tag{9.134}$$

Invert the above equation to obtain

$$\lambda_1^{(n)} = \frac{\sqrt{(1 - 2e_{22}^{(n)})}}{\sqrt{[(1 - 2e_{11}^{(n)})(1 - 2e_{22}^{(n)}) - 4(e_{12}^{(n)})^2]}}$$

$$\lambda_2^{(n)} = \frac{1}{\sqrt{(1 - 2e_{22}^{(n)})}} \tag{9.135}$$

$$K^{(n)} = \frac{2e_{12}^{(n)}}{1 - 2e_{22}^{(n)}}$$

where $\lambda_1^{(n)}$ and $\lambda_2^{(n)}$ are the extension ratios of the sub-element (n) in the longitudinal and transverse directions, respectively; and $K^{(n)} = \tan \Phi^{(n)}$ as shown in Fig. 9.22. The current fiber orientation is obtained from Eq. (9.129). Then, $\lambda_1^{(n)}$, $\lambda_2^{(n)}$, and $K^{(n)}$ can be determined by an iterative calculation from Eqs. (9.106), (9.131) and (9.134). Also, the average extension of a wavelength in the longitudinal direction, λ_1, can be determined by Eq. (9.130).

The predictions of the longitudinal constitutive relations based upon the Lagrangian and Eulerian approaches are compared to experimental results and an incremental analysis in the finite deformation range (Luo, Kuo and Chou 1988). The model composite system consists of silicone elastomer reinforced with sinusoidally shaped Kevlar fibers ($a/\lambda = 0.09$). Due to fiber waviness, the volume fraction may vary among the sub-elements. An average fiber volume fraction $V_f = 9\%$ is used in the calculation. Also, the elastic constants are given in Table 9.1. Figure 9.24 compares the analytical predictions with experimental results. The heavy solid line indicates theoretical predictions of the Lagrangian approach (Luo and Chou 1988b, 1990b); the thin solid line indicates theoretical predictions based upon the Eulerian approach (Luo and Chou 1988a, 1990a); and the dotted line is from the incremental analysis (Kuo, Takahashi and Chou 1988). Experimental results are also presented.

Furthermore, the local strains in the sub-element can be predicted directly from Eqs. (9.127). The current fiber orientation angle of the sub-element is given by Eq. (9.129). These results show that the maximum local tensile strain of the fiber occurs at the

Fig. 9.24. Stress–strain relations of Kevlar/silicone elastomer composite laminae containing sinusoidally shaped fibers for $a/\lambda = 0.09$. (After Luo and Chou 1990b.)

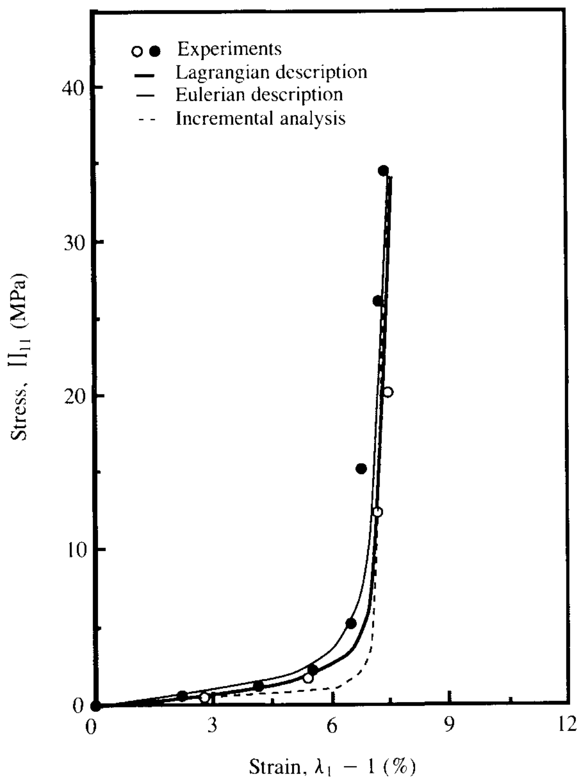

region where the initial fiber orientation angle equals zero (i.e. $X_1 = \pm\lambda/4$). The maximum local shear strain of the composites occurs in the region where the initial fiber orientation is a maximum (i.e. $X_1 = 0$, $\lambda/2$). Hence, the strength of the flexible composites may be determined by the maximum tensile strain at $X_1 = \lambda/4$ and the maximum shear strain at $X_1 = 0$.